Stephen McCarthy; Dmitrii Rachinskii
Dynamics of systems with Preisach memory near equilibria

Mathematica Bohemica, Vol. 139 (2014), No. 1, 39–73

Persistent URL: `http://dml.cz/dmlcz/143636`

139 (2014) MATHEMATICA BOHEMICA No. 1, 39–73

DYNAMICS OF SYSTEMS WITH PREISACH MEMORY NEAR EQUILIBRIA

Stephen McCarthy, Cork, Dmitrii Rachinskii, Dallas

(Received August 12, 2012)

Abstract. We consider autonomous systems where two scalar differential equations are coupled with the input-output relationship of the Preisach hysteresis operator, which has an infinite-dimensional memory. A prototype system of this type is an LCR electric circuit where the inductive element has a ferromagnetic core with a hysteretic relationship between the magnetic field and the magnetization. Further examples of such systems include lumped hydrological models with two soil layers; they can also appear as a component of the recently proposed models of population dynamics. We study dynamics of such systems near an equilibrium point. In particular, we show and examine a similarity in the behaviour of trajectories between the system with the Preisach memory operator and a planar slow-fast ordinary differential equation. The nonsmooth Preisach operator introduces a singularity into the system. Furthermore, we classify the robust equilibrium points according to their stability properties. Conditions for stability, instability and partial stability are presented. A robust partially stable point simultaneously attracts many trajectories and repels many trajectories (a behaviour which is not generic for smooth ordinary differential equations). We discuss implications of such local dynamics for the excitability properties of the system.

Keywords: return-point memory; Preisach operator; oscillator with memory; hysteresis; operator-differential equation; stability of equilibrium; partial stability; slow-fast system; switching line; excitability

MSC 2010: 34C55, 47J40

1. Introduction

Hysteresis effects underpin modern magnetic recording technologies and should be taken into account in microelectromechanical systems (MEMS) engineering. They can also manifest themselves through undesirable energy losses in electronic circuits,

This publication has emanated from research conducted with the financial support of the Alexander von Humboldt Foundation, Germany and the Russian Foundation for Basic Research, grant 10-01-93112.

mechanical and other systems, where hysteresis can be a primary or significant source of energy dissipation. Mathematical models of systems with hysteretic components help design power electronic systems [57]; implement real time hysteresis compensation in controllers and actuators [40], [59], [19], [31]; design smart materials [9], [4], [23]; model and predict dynamics of earthquakes faults [18] and phase transitions [54], [5]; understand dynamics of complex networks [27], [10].

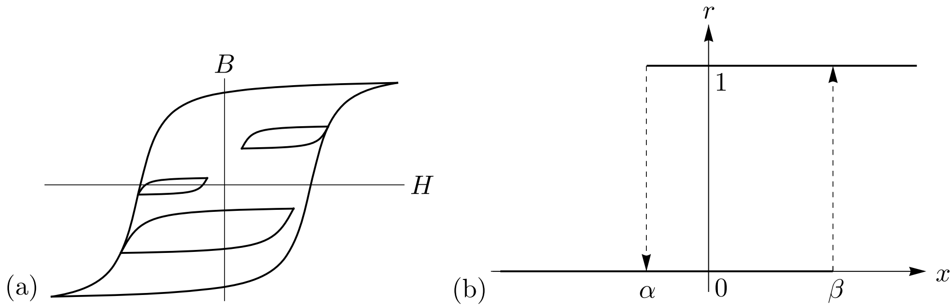

Figure 1. (a) Hysteresis loops in relationship between external magnetic field H and magnetic induction B of a ferromagnetic material. (b) Input-output diagram of the non-ideal relay with thresholds α, β.

A hysteretic constitutive relationship between variables, such as the relationship between a magnetic field H and magnetic induction B in ferromagnetic materials presented by nested hysteresis loops on H-B diagrams, see Figure 1 (a), or the constitutive relationship between stress and strain variables in elastoplastic materials, is described by an operator in mathematical terms [43], [34]. Such operators share a number of common basic properties including the property of rate-independence, which is often used as the definition of a hysteresis operator[1] [58], causality, semigroup property and nonsmoothness. Hence, modelling of systems which involve components with a hysteretic relationship between input and output naturally leads to differential equations coupled with an operator relationship between some of the variables. This rather general approach to modelling such systems[2] can be illustrated by an electrical circuit where an inductance element contains a ferromagnetic core (for example, a transformer). Kirchhoff's laws (or Maxwell's equations) lead to differential rate equations for voltages and currents; those are complemented by constitutive relationships, which, in case of a hysteretic ferromagnetic core, include an operator relationship between the fields H and B in the core where H is propor-

[1] It is the property of rate-independence that underpins a familiar description of hysteresis in terms of input-output diagrams such as in Figure 1 (a).

[2] Alternative models of systems with hysteresis include differential inclusions, variational inequalities and other models based on the variational approach.

tional to the current and B is proportional to the rate of change of the voltage [57], [36], [24].

As a prototypical example consider the LCR circuit where the inductance element has a ferromagnetic core. If there is no hysteresis effect, or this effect can be neglected, then, in the simplest case, B is proportional to H in the core and the emf in the inductor can be expressed as

$$E_{\text{ind}} = Lj' \tag{1.1}$$

where prime denotes the time derivative and j is the current through the inductor. Hence the dynamics of the current j and the drop of the voltage u across the capacitor are described by the system

$$Lj' = -Rj + u, \quad Cu' = -j. \tag{1.2}$$

However, if the hysteresis effect is substantial, then the constitutive relationship between B and H is not only nonlinear, but the instantaneous value of B depends both on the simultaneous value of H and some previous values of H. The Preisach operator is a widely used model of hysteretic constitutive relationship in ferromagnetic materials [30], [44]. Adopting this model of the relationship between the magnetization M and the magnetic field H results in the equation

$$B = \nu H + P(H) \tag{1.3}$$

with $\nu > 0$ where the Preisach input-output operator P maps the time series of the magnetic field $H(t)$ to the time series of the magnetization $M(t) = (P(H))(t)$ of the core. This leads to a similar expression for the emf induced in the inductor

$$E_{\text{ind}} = (Lj + P(j))' \tag{1.4}$$

where the Preisach operator density function is properly rescaled when we pass from (1.3) to (1.4). When the linear functional relationship (1.1) is replaced with (1.4), system (1.2) changes accordingly to the system of differential equations

$$(Lj + P(j))' = -Rj + u, \quad Cu' = -j \tag{1.5}$$

involving the Preisach hysteresis operator P.

System (1.5) is a functional differential equation with an infinite dimensional phase space as the rates of change of the variables depend both on the simultaneous values of the variables and, through the operator P, on their values in the past. Importantly, the rate-independence property of the operator P distinguishes the memory in this system from other types of memory such as in delay differential equations or convolution operators. Rate-independence implies that shock values of the variable j have permanent effect on the output in the future, accounting for the fact that the ferromagnetic material remains permanently magnetized even after the magnetic field H, which has created the magnetization, has been removed. More precisely, the memory stack of system (1.5) at any time t consists of a sequence of certain extremum values of j achieved prior to the instant t (the so-called sequence of main extremum values of j). Equations (1.5) define how the rates j', u' depend on the simultaneous values of j, u and the first element of the memory stack which changes each time the memory gets updated; this memory element defines the B-H curve followed by the system at a given time from infinitely many possible curves passing through each point of the input-output diagram in Figure 1 (a). The memory stack is dynamically updated (a) at turning points of j where j' changes sign; and, (b) whenever j reaches the value of the second element of the memory stack. Either of these events causes the system to switch to another B-H branch on the input-output diagram; more details will be given in the next section.

As oscillating contours and elements, including those with hysteretic components, are a common feature of various electrical circuits, mechanical systems and MEMS, several prototypical second order differential models of oscillators with the Preisach operator have been proposed and studied in engineering and mathematical literature. In particular, various aspects of dynamics of forced oscillators have been studied in [39], [22], [6], [41], [42], [32], [55], [60], [56], [7], including applications to accurate modelling and optimization of parameters of power electronics systems in the presence of the ferroresonance phenomenon [57] and input-to-state stability of control systems. Cycles stemming from the Hopf bifurcation in a model of Van der Pol type oscillator, a network of such oscillators and other systems with hysteresis were studied in [1], [3], [33], [20], [21]. In the electrical circuitry context, this model describes a circuit consisting of an LCR contour and a negative feedback loop (which can be implemented, for instance, by using tunnel diodes) and involving a ferromagnetic core in the inductor. The model equations

$$(Lj + P(j))' = -Rj + u, \quad Cu' = -j + \sigma_1 u - \sigma_2 u^3, \tag{1.6}$$

when compared to (1.5), include additionally the current-voltage characteristic $j_d = -\sigma_1 u + \sigma_2 u^3$ of the negative feedback element with $\sigma_1 > 0$ and $\sigma_2 \geqslant 0$.

In this paper, we consider a general class of second order systems of differential equations

$$\begin{aligned} (Px)' &= f(x, y), \\ y' &= g(x, y) \end{aligned} \tag{1.7}$$

with the Preisach operator P. We focus on dynamics of the system near an equilibrium point such as, for example, the zero equilibrium of system (1.5) or system (1.6). In the context of this local problem, it is important that systems (1.5) and (1.6) have the form (1.7) for $L = 0$. This corresponds to the physical approximation $Lj \ll P(j)$ which is typical of the inductors where almost all the magnetic flux is concentrated in the ferromagnetic core. Thus, we consider system (1.7) as a natural approximation of electrical circuit models such as (1.5) and (1.6). Further examples motivating the analysis of system (1.7) and its extensions in the context of hydrology and other applications will be presented in Section 3. Mathematically, the term Lj' with $L > 0$ in equations (1.5), (1.6) has a smoothing effect, see [37], [38].

The goal of this paper is to study local stability of an equilibrium of system (1.7). Although the system is infinite-dimensional, the projection of dynamics on the (x, y) plane plays the main role for stability analysis. From the two memory effects mentioned above, the turning points of the x component of a solution affect the dynamics near an equilibrium substantially; the effect of points where the x component crosses its previous extremum values is either not there at all or less important. As the turning points are located on the line $f(x, y) = 0$, it plays an important role, which is somewhat similar to the role of a switching line in control systems theory. We will see that system (1.7) has a singularity on the line $f = 0$ due to the fact that the memory stack is updated each time the projection of a trajectory on the (x, y) plane crosses this line.

The paper is organized as follows. In the next section, we discuss the Preisach operator and some properties of the Cauchy problem for system (1.7). Section 3 contains main results. Theorems 3.1–3.4 describe trajectories which cross the line $f = 0$ near an equilibrium of system (1.7). Such trajectories can follow the line $f = 0$ to, or from, the equilibrium, or escape its neighbourhood along the x-direction. This behaviour is somewhat similar to that of a slow-fast ordinary differential system with the fast variable x. We discuss the singularity of system (1.7) on the line $f = 0$, which is the origin of this similarity, and present numerical examples. Theorems 3.2–3.4 are used later to analyse the stability of the equilibrium point. Stability results are summarised in Theorem 3.5. In particular, system (1.7) can have a robust equilibrium point, which we call partially stable. Such an equilibrium is characterized by the property that it, simultaneously, attracts many trajectories and repels many trajectories; a rigorous definition will be presented. This property can potentially result in the excitable behaviour of the system if the global dynamics can glue repelled and attracted trajectories [35], [29]. We discuss this possibility; however, an explicit example remains an open problem, as global dynamics is beyond the scope of this paper. Finally, we briefly discuss possible extensions of Theorems 3.2–3.4 to systems with $n > 2$ phase variables obtained by a singular perturbation of equations (1.7).

Proofs are presented in Section 4. For simplicity, in the formulations and proofs of the stability results we restrict ourselves to a certain natural class of initial states of the Preisach operator.

2. Preliminaries

2.1. Preisach memory model. The Preisach operator is a classical model of complex hysteretic constitutive relationships in magnetism, plasticity, sorption, piezoelectricity, phase transitions and other physics disciplines; more recently, it has found applications in macroeconomic, epidemiological and ecological modelling. Here the wording 'complex hysteresis' means that an oscillating input of any small amplitude generates a hysteresis loop (which, in the context of physics problems, is associated with energy dissipation). The Preisach model is based on simple phenomenology describing the input-output relationship in terms of its decomposition into elementary two-state memory operators, the so-called non-ideal relays.

The non-ideal relay (also known as non-ideal switch, lazy switch, or Schmidt trigger) is the simplest hysteretic transducer, characterized by threshold values α, β where $\alpha < \beta$. The input of this transducer is a continuous scalar function $x(t)$; the output $r(t)$, at any moment in time, can take one of the two values, 0 (the relay is 'off') or 1 (the relay is 'on'). Moreover, the input-output pair $(x(t), r(t))$ always belongs to the union of the two thick black lines $\Omega = \{(x, r)\colon\, x < \beta, r = 0\} \cup \{(x, r)\colon\, x > \alpha, r = 1\}$ in Figure 1 (b). If at some moment t the output is $r(t) = 0$ (hence, $x(t) < \beta$), then the output will remain zero until the first moment $t' > t$ when the input reaches the threshold value $x(t') = \beta$. At this moment, the output switches to the value $r(t') = 1$. Similarly, if $r(t) = 1$ (hence, $x(t) > \alpha$) at a moment t, then the output remains equal to 1 till the first moment $t' > t$ when the input reaches the threshold value $x(t') = \alpha$; at this moment, the output switches to the value $r(t') = 0$. Given a continuous input $x(t), t \geqslant t_0$ and an initial value of the input $r(t_0) = r_0$ such that $(x(t_0), r(t_0)) \in \Omega$, these two simple rules define the binary output $r(t), t \geqslant t_0$ of the non-ideal relay. We will denote this output by

$$r(t) = (\mathcal{R}_{\alpha,\beta}[r_0]x)(t). \tag{2.1}$$

Note that if $\alpha < x(t_0) < \beta$, then each of the two initial conditions $r_0 = 0, 1$ is possible, and they define different outputs for the same input.

In the formalism of the Preisach model, one considers a collection of non-ideal relays, which all respond independently to the same continuous input $x(t)$, $t \geqslant t_0$. The outputs of the relays are then weighted to obtain the output of the system. Each relay is identified by a different pair of thresholds (α, β), which ranges over a subset

Π of the half-plane $\alpha < \beta$ (the so-called Preisach half-plane). For our purposes, it is convenient to define Π to be a strip $\Pi = \{(\alpha, \beta)\colon\ \alpha \leqslant \beta \leqslant \alpha + d\}$. Given an initial value $r_0(\alpha, \beta) \in \{0, 1\}$ for each $(\alpha, \beta) \in \Pi$, formula (2.1) defines the output

$$r(t; \alpha, \beta) = (\mathcal{R}_{\alpha,\beta}[r_0(\alpha, \beta)]x)(t), \quad t \geqslant t_0 \tag{2.2}$$

of each relay contributing to the system. The output of the whole system is then defined by the integral

$$p(t) = \int_\Pi \mu(\alpha, \beta) r(t; \alpha, \beta)\, \mathrm{d}\alpha\, \mathrm{d}\beta = \int_\Pi \mu(\alpha, \beta)(\mathcal{R}_{\alpha,\beta}[r_0(\alpha, \beta)]x)(t)\, \mathrm{d}\alpha\, \mathrm{d}\beta \tag{2.3}$$

over all the relays, where the nonnegative weighting function $\mu\colon \Pi \to \mathbb{R}$ is called the Preisach density function; it is assumed to be continuous, uniformly bounded and integrable over the strip Π. Although the outputs of individual relays (2.2) are binary and hence, generically, discontinuous, the output $p(t)$, $t \geqslant t_0$ of the Preisach model is continuous due to weighting [5], [34], [43].

2.2. Evolution of states. The function $r(t; \cdot, \cdot)\colon \Pi \to \{0, 1\}$, describing the outputs of all the relays at a moment t, is called the state of the Preisach model at this moment. In particular, $r(t_0; \cdot, \cdot) = r_0(\cdot, \cdot)$ is an initial state. Thus, equation (2.3) defines the evolution of the state in time for given input and initial state. However, this evolution can be described in simpler geometrical terms [34], [43].

From all the possible states of the Preisach model, we will consider a smaller natural class of states of a special form, see Figure 2. Here, there is a staircase polyline S that divides the strip Π on the (α, β) plane into two parts. The state $r(\alpha, \beta)$ of the Preisach model equals 1 below the polyline S and equals 0 above the polyline S. The polyline S consists of either a final or countable number of vertical and horizontal segments; in the latter case, the only accumulation point of the corners of the polyline is its end located at the bisector $\alpha = \beta$.

The polyline $S = S(t)$, separating the domain where $r(t; \alpha, \beta) = 1$ (the area shaded dark in Figure 2) from the domain where $r(t; \alpha, \beta) = 0$ (white) on the Preisach half-plane, changes in response to the variation of the input $x(t)$. Formula (2.2) defines the following rules of evolution of $S = S(t)$. The right end of S at the bisector $\alpha = \beta$ always has the coordinates equal to $x(t)$. Imagine that the input $x = x(t)$ moves along the horizontal axis and controls the right end $(x(t), x(t))$ of $S(t)$ on the diagonal $\alpha = \beta$. When $x(t)$ increases, the point $(x(t), x(t))$ on the diagonal drags the horizontal line and colors the domain below this line and above the diagonal. For instance, if, in Figure 2 (a), x increases from the value x_0 to the value $\tilde{x}$, the colored area is increased by the lightly shaded triangle. When $x(t)$ decreases, the diagonal

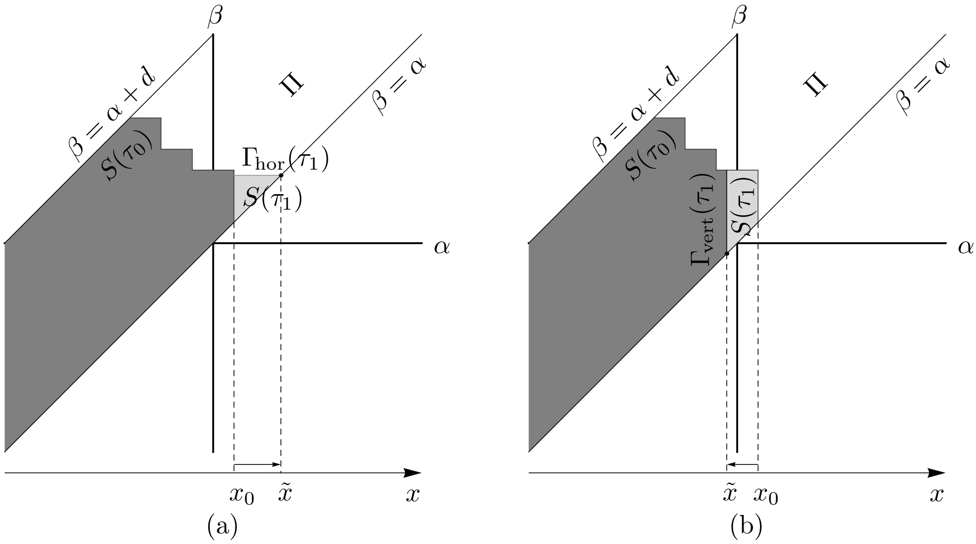

Figure 2. Evolution of a varying state of the Preisach model. In the colored domain $\Omega(S(t))$ the relays are on, in the white domain they are off. The output $p(t)$ of the model is the area of the colored domain with respect to the density μ.

point drags the vertical line, and colors in white everything to the right of this line and above the diagonal as in Figure 2 (b), where the coloured area decreases by the lightly shaded trapezium as the input x decreases from the value x_0 to $\tilde{x}$.

If we denote by $\Omega(S(t))$ the part of the strip Π below (to the left of) the polyline $S(t)$, that is the domain where $r(t;\alpha,\beta) = 1$, then the output (2.3) of the Preisach model is the area of $\Omega(S(t))$ with respect to the density μ,

$$p(t) = \int_{\Omega(S(t))} \mu(\alpha,\beta)\, \mathrm{d}\alpha\, \mathrm{d}\beta. \tag{2.4}$$

In what follows, the polyline $S = S(t)$ is referred to as the staircase state (or, just the state) of the Preisach model at the moment t, as it defines the output $p(t)$ of the model according to formula (2.4), and the outputs $r(t;\alpha,\beta)$ of the individual relays. We will use the notation P for the Preisach operator that maps a pair $(x(t), S_0)$, where $x(t)$ is a continuous input defined on a time interval $[t_0, t_1)$ (or, $[t_0, t_1]$) and $S_0 = S(t_0)$ is an initial staircase state of the Preisach model, to the continuous output (2.4) defined on the same time interval as the input,

$$p(t) = (P[S_0]x)(t). \tag{2.5}$$

This is the operator (2.3) when we restrict our attention to the staircase states. If we introduce the Hausdorff metric $\varrho(\cdot,\cdot)$ between the staircase polylines S and the uniform metric in the spaces of inputs and output, then the Preisach operator is globally Lipschitz continuous,

$$\|p_1 - p_2\|_{C[t_0,t_1]} \leqslant K(\|x_1 - x_2\|_{C[t_0,t_1]} + \varrho(S_1(t_0), S_2(t_0)))$$

where $p_i(t) = (P[S_i(t_0)]x_i)(t)$ and the Lipschitz constant K is the same for any time interval $[t_0, t_1]$. A similar estimate, with the same right hand side, holds for the maximal distance $\max_{t_0 \leqslant t \leqslant t_1} \varrho(S_1(t), S_2(t))$ between the staircase states varying in response to the variation of the inputs x_i. The domain of the Preisach operator (2.5) consists of pairs $(x(t), S(t_0))$ such that the right end of the staircase state S_0, which is situated on the bisector $\alpha = \beta$, is placed at the point $(x(t_0), x(t_0))$. We will always assume that this compatibility between the initial staircase state and the initial value of the input is respected, meaning by 'any initial state' an arbitrary state with the right end at the point $(x(t_0), x(t_0))$.

An important notice for the following is that if the input $x(t)$ strictly increases on any time interval $[\tau_0, \tau_1]$, then the staircase state $S(\tau_1)$ at the moment τ_1 has a finite number of corners and links, and the link connecting the right end of the polyline $S(\tau_1)$ to the next corner is *horizontal*. We call this link the *initial* link, or the initial segment, of the staircase state, see Figure 2. Furthermore, if the input $x(t)$ strictly decreases on any time interval $[\tau_0, \tau_1]$, then the staircase state $S(\tau_1)$ also has a finite number of corners and links, but the initial segment is *vertical*. In particular, for any piecewise monotone input, $S(t)$ has a finite number of corners and links at any moment. For an input $x(t)$, which strictly increases on a time interval $[\tau_0, \tau_1]$, the initial link of the state $S(\tau_1)$ is the horizontal segment connecting the point $(x(\tau_1), x(\tau_1))$ with the staircase state $S(\tau_0)$. That is, setting $S_0 = S(\tau_0), x_0 = x(\tau_0), \tilde{x} = x(\tau_1)$ and denoting by $(\tilde{\alpha}_{S_0}(\tilde{x}), \tilde{x})$ the most right intersection point of the horizontal line $\beta = \tilde{x}$ with the staircase polyline S_0 (or, in case they do not intersect, defining $(\tilde{\alpha}_{S_0}(\tilde{x}), \tilde{x})$ as the intersection point of the line $\beta = \tilde{x}$ with the upper boundary of the strip Π), the initial horizontal segment of the state $S(\tau_1)$ is

$$\Gamma_{\text{hor}} = \{(\alpha, \beta)\colon\ \tilde{\alpha}_{S_0}(\tilde{x}) \leqslant \alpha \leqslant \tilde{x},\ \beta = \tilde{x}\}, \quad \tilde{x} \geqslant x_0,$$

see Figure 2. Similarly, for an input $x(t)$, which strictly decreases on a time interval $[\tau_0, \tau_1]$, the initial vertical link of the state $S(\tau_1)$ connects the point $(x(\tau_1), x(\tau_1)) = (\tilde{x}, \tilde{x})$ to the staircase $S_0 = S(\tau_0)$. That is, denoting by $(\tilde{\beta}_{S_0}(\tilde{x}), \tilde{x})$ the lowest intersection point of the vertical line $\alpha = \tilde{x}$ with the staircase polyline S_0 (or, if they do not intersect, the intersection point of the line $\alpha = \tilde{x}$ with the upper boundary of the strip Π), the initial vertical segment of the state $S(\tau_1)$ is

$$\Gamma_{\text{ver}} = \{(\alpha, \beta)\colon\ \tilde{x} \leqslant \beta \leqslant \tilde{\beta}_{S_0}(\tilde{x}),\ \alpha = \tilde{x}\}, \quad \tilde{x} \leqslant x_0.$$

For analysis of system (1.7), the integral of the Preisach density function over the initial segment of the staircase state plays an important role. The reason for this is that the above law of evolution of the staircase state $S(t)$ and the formula (2.4) for the output lead to the relationship

$$p'(t) = L_{S_0}(x(t))x'(t), \tag{2.6}$$

where the function $L_{S_0}\colon \mathbb{R} \to \mathbb{R}$ is defined by

$$L_{S_0}(\tilde{x}) = \begin{cases} \displaystyle\int_{\alpha_{S_0}(\tilde{x})}^{\tilde{x}} \mu(\alpha, \tilde{x})\,\mathrm{d}\alpha, & \tilde{x} \geqslant x_0, \\ \displaystyle\int_{\tilde{x}}^{\beta_{S_0}(\tilde{x})} \mu(\tilde{x}, \beta)\,\mathrm{d}\beta, & \tilde{x} \leqslant x_0. \end{cases} \tag{2.7}$$

More precisely, if $S(\tau_0) = S_0$, $x(\tau_0) = x_0$, the input $x(t)$ is monotone on a time interval $[\tau_0, t]$, the derivative x' is defined at the moment t, and $\tilde{x} = x(t)$ is a point of continuity of the function (2.7), then the output p is differentiable at the moment t and its derivative is defined by the formula (2.6). The function $L_{S_0} = L_{S_0}(\tilde{x})$ is continuous except for points $\tilde{x}$ where $\tilde{x}$ equals either an abscissa or an ordinate of a corner of the staircase polyline S_0; at each discontinuity point, L_{S_0} makes a finite jump. Further discussion of the Preisach operator can be found, for example, in [5].

2.3. Differential system with Preisach memory. In the framework of dynamical systems theory, a solution has three components, $(x(t), y(t), S(t))$. That is, the phase space of system (1.7) is the space of triplets (x, y, S). In particular, the Cauchy problem for equation (1.7) consists in finding a solution satisfying a given initial condition $(x(t_0), y(t_0), S(t_0)) = (x_0, y_0, S_0)$. Due to the semigroup property of the Preisach operator [34], one can merge two solutions defined on consecutive time intervals $[t_0, t_1]$ and $[t_1, t_2]$ to form a solution on the time interval $[t_0, t_2]$ if the final point $(x(t_1), y(t_1), S(t_1))$ of the solution defined on the interval $[t_0, t_1]$ coincides with the initial point of the solution defined on the interval $[t_1, t_2]$. In this way, the usual continuation procedure works for system (1.7). We note the rate-independence property of the Preisach operator implies that this operator commutes with the group of translations of time. Therefore, system (1.7) is autonomous.

In what follows, we will use the term solution in relation to a triplet $(x(t), y(t), S_0)$ or, whenever an initial state S_0 is either fixed or can be chosen arbitrarily from the set of all admissible initial states of the Preisach operator, to the pair $(x(t), y(t))$. We note that the evolution of the state $S(t)$ of the Preisach operator is uniquely defined by the initial state S_0 and the input $x(t)$ of this operator according to the definition of the previous section, hence it is legitimate to consider triplets $(x(t), y(t), S_0)$ instead of $(x(t), y(t), S(t))$.[3] The projection of solutions on the (x, y)-plane plays the main role for the results presented below.

For a given initial state S_0, a pair $(x(t), y(t))$, $t \in [t_0, t_1)$ is a solution of system (1.7) if the output $p(t) = (P[S_0]x)(t)$ of the Preisach operator and the component $y(t)$ are continuously differentiable, the component $x(t)$ is continuous, and equations (1.7) are satisfied at all points of the interval $[t_0, t_1)$.

A stationary solution of system (1.7) is a solution satisfying $(x(t), y(t)) \equiv (x_0, y_0)$. As the Preisach operator maps a constant input to a constant output, the component $S(t)$ of a stationary solution and the output $p(t) = (P[S_0]x)(t)$ of the Preisach operator are also constant, $S(t) \equiv S_0$, $p(t) \equiv p_0$. Therefore, as in the case of ordinary differential equations, for any stationary solution $(x(t), y(t)) \equiv (x_0, y_0)$,

$$f(x_0, y_0) = g(x_0, y_0) = 0. \tag{2.8}$$

Moreover, relations (2.8) imply that $(x(t), y(t)) \equiv (x_0, y_0)$ is a stationary solution of system (1.7) for any initial state S_0 of the Preisach operator. Hence, we call a solution (x_0, y_0) of equations (2.8) an *equilibrium* of system (1.7).

Our focus will be on the dynamics near an isolated equilibrium. Without loss of generality, we assume that the equilibrium is placed at the origin. Results will be formulated in terms of the Jacobian matrix

$$Q = \begin{pmatrix} f_x(0,0) & f_y(0,0) \\ g_x(0,0) & g_y(0,0) \end{pmatrix} \tag{2.9}$$

evaluated at the zero equilibrium, where f_x, f_y, g_x, g_y are the partial derivatives of the functions f and g, which are assumed to be continuously differentiable. We assume the non-degeneracy condition

$$j_0 = \det Q \neq 0, \tag{2.10}$$

which ensures that the zero equilibrium $(x_0, y_0) = (0, 0)$ is isolated.

2.4. Cauchy problem. The properties of the Cauchy problem for system (1.7) depend on the properties of the Preisach density function μ. We will assume that the continuous nonnegative function μ is positive on the line $\alpha = \beta$. In this case, for any given initial state S_0, the Preisach operator $P[S_0]$ maps the space of all inputs $x \in C[t_0, t_1]$ satisfying an initial condition $x(t_0) = x_0$ to an open subset $\mathfrak{D}$ of the space of continuous outputs $p \in C[t_0, t_1]$ satisfying the initial condition $p(t_0) = p_0$, where $p_0 = p_0(S_0)$ is defined by S_0, and we use the uniform norm in the spaces of inputs

[3] In applications, S is typically not an observable variable.

and outputs. Moreover, this operator has a continuous inverse $P^{-1}[S_0]$ defined on $\mathfrak{D}$. The existence of this inverse operator ensures the local existence of a solution to the Cauchy problem. That is, for any initial data $(x(t_0), y(t_0), S(t_0)) = (x_0, y_0, S_0)$, system (1.7) has a solution on a sufficiently small interval $[t_0, t_1]$. The existence can be proved by replacing (1.7) with the equivalent system

$$\begin{aligned}
&p'(t) = f((P^{-1}[S_0]p)(t), y(t)),\\
&y'(t) = g((P^{-1}[S_0]p)(t), y(t)),\\
&p(t_0) = p_0, \quad y(t_0) = y_0
\end{aligned}$$

where $p(t) = (P[S_0]x)(t)$, and then passing to the integral equation equivalent to this system. The Schauder fixed point principle ensures the existence of a solution to the integral equation on a sufficiently small time interval $[t_0, t_1]$ in a standard way (details can be found, for example, in [6]). As the continuation argument applies to solutions of system (1.7), every solution can be extended from an interval $[t_0, t_1]$ to a maximal interval of existence $[t_0, T)$ where $T \leqslant \infty$. Moreover, a standard argument can be adapted from the theory of ordinary differential equations to show that if the interval $[t_0, T)$ is finite, then $|x| + |y| \to \infty$ as $t \to T-$.

Uniqueness of solutions is a more complicated problem. First, we note that, given initial data $(x(t_0), y(t_0), S(t_0)) = (x_0, y_0, S_0)$, a solution of the Cauchy problem may be unique on a time interval $[t_0, t_1]$, but it cannot be uniquely extended in backward time. This is an effect of the memory in the system. Indeed, given a state S_0 of the Preisach operator at a moment t_0 and an input $x(t)$ on a time interval $[t_-, t_0]$ preceding the moment t_0, the state and output of the Preisach operator are not uniquely defined on any time interval $[\tau, t_0]$. As a consequence, one can show that an attempt to extend a solution of system (1.7) in backward time from a point $(x(t_0), y(t_0), S(t_0))$ in the phase space leads to non-uniqueness at every point $t < t_0$. Therefore, a solution of the Cauchy problem is considered for $t > t_0$ only.

Next, let us show the forward uniqueness of solutions in the domain where $f(x, y) \neq 0$. If a solution satisfies $f(x(t), y(t)) > 0$ on some interval (t_0, t_1) (or, $[t_0, t_1)$), then the output $p(t) = (P[S(t_0)]x)(t)$ and the input $x(t) = (P^{-1}[S(t_0)]p)(t)$ of the Preisach operator both strictly increase on this time interval, as $p'(t) = f(x(t), y(t)) > 0$. Therefore, on any subinterval $[\tau, \tau + \Delta]$ of this time interval, the initial segment of the state $S(t)$ is horizontal and the function $L(\tilde{x}) = L_{S(t_0)}(\tilde{x})$ defined by (2.7) is positive, separated from zero, piecewise continuous, and continuously differentiable between its discontinuity points $\tilde{x}_k$ at which $L(\tilde{x})$ has finite jumps (where $\tilde{x}_k$ are the ordinates of the corners of the state $S(t_0)$). Hence, the relation $p' = L(x)x'$ implies that the solution of system (1.7) satisfies the ordinary differential system

$$L(x)x' = f(x, y), \quad y' = g(x, y) \tag{2.11}$$

on the interval $[\tau, \tau + \Delta]$. Due to the above properties of the function L, a solution of system (2.11) with any initial data from the domain $f(x, y) > 0$ is uniquely extendable in forward time as long as it remains in this domain (details can be found in [37]). Hence, if $f(x_0, y_0) > 0$ and the initial state S_0 has a horizontal initial segment, then the solution of the Cauchy problem for equation (1.7) with the initial data $(x(t_0), y(t_0), S(t_0)) = (x_0, y_0, S_0)$ is uniquely extendable in forward time as long as the point $(x(t), y(t))$ remains in the domain $f(x, y) > 0$ of positivity of f. A similar argument proves the forward uniqueness of solutions of system (1.7) in the domain $f(x, y) < 0$ provided that $f(x(t_0), y(t_0)) < 0$ and the initial segment of the initial state $S(t_0)$ is now vertical. Such a solution also satisfies the ordinary differential system (2.11).

Thus, the potential locus of forward non-uniqueness is the line $f(x, y) = 0$. The following example shows that the non-uniqueness is indeed possible.

E x a m p l e 1. Consider the system

$$(Px)' = x, \quad y' = -y \tag{2.12}$$

where the equations are decoupled. The forward non-uniqueness is due to the x-equation; the second equation can be replaced by any equation $y' = g(x, y)$.

Consider an initial data set $x(t_0) = 0, y(t_0) = y_0, S(t_0) = S_0$, where the equality $x(t_0) = 0$ ensures that the initial point lies on the line $f = 0$. The Cauchy problem with this initial data has a solution $x(t) = 0$, $y(t) = y_0 \mathrm{e}^{-(t-t_0)}$, $S(t) = S_0$, $t > t_0$ with the stationary x-component and the stationary Preisach operator state. At the same time, if we assume that the Preisach operator density function is constant, $\mu(\alpha, \beta) = \mu_0 = 1$, in some neighbourhood of the point $\alpha = \beta = 0$ and that the initial state S_0 has a nonzero vertical initial segment, then the function L in (2.11) equals $L(x) = x$ in some right neighbourhood of the point $x = 0$. Hence, the ordinary differential system (2.11) reads

$$xx' = x, \quad y' = -y$$

for $x \geqslant 0$, and its solution $x = t - t_0$, $y = y_0 \mathrm{e}^{-(t-t_0)}$ is, simultaneously, another solution of the same Cauchy problem for system (1.7) for $t \geqslant t_0$. Combining the two solutions, we obtain a continuum of solutions of this Cauchy problem for system (1.7), which all have the same y-component, but different x-component

$$x(t)=0 \quad \text{for } t_0 \leqslant t \leqslant t_0+\Delta; \quad x(t)=t-t_0-\Delta \quad \text{for } t>t_0+\Delta$$

with an arbitrary $\Delta \geqslant 0$. A similar argument shows that, if the initial state S_0 has a nonzero horizontal initial segment, then the same Cauchy problem has a continuum of solutions with the x-component

$$x(t)=0 \quad \text{for } t_0 \leqslant t \leqslant t_0+\Delta; \quad x(t)=-(t-t_0-\Delta) \quad \text{for } t>t_0+\Delta.$$

Note that the initial point in this example can be the zero equilibrium $x_0=y_0=0$ of the system.

Example 2. The backward non-uniqueness means that solutions of system (1.7) starting from different initial conditions at $t=t_0$ can merge at $t>t_0$. It is easy to show the backward non-uniqueness of solutions in the domain $f(x,y)>0$ (or, $f(x,y)<0$). Here we consider an example where a solution merges with the equilibrium after infinitely many crossings of the line $f=0$.

Let us consider the system

$$(Px)'=-y, \quad y'=x \tag{2.13}$$

where the Preisach operator density function is constant, $\mu=\mu_0>0$, in a neighbourhood of the point $\alpha=\beta=0$. Assume the initial conditions $x(0)=x_0>0$, $y_0=0$ and the horizontal initial state S_0 of the Preisach model. A trajectory of equations (2.13) on the (x,y)-plane, which starts from these initial conditions, can be found explicitly from equations (2.11). This is a spiral which consists of infinitely many arcs l_n, $n\geqslant 1$, converging to the zero equilibrium, where each arc l_n is a trajectory of the system

$$(-1)^{n-1}(x_{n-1}-x)\mu_0 x'=-y, \quad y'=x, \tag{2.14}$$

connecting points $(x_{n-1},0)$ and $(x_n,0)$ of the x-axis. Excluding time, one obtains the equation $\mu_0(-1)^{n-1}(x_{n-1}-x)x\,\mathrm{d}x+y\,\mathrm{d}y=0$ for l_n, which leads to the solution

$$l_1=\left\{(x,y)\colon\ y=(x_0-x)\sqrt{\frac{\mu_0}{3}(x_0+2x)},\ -\frac{x_0}{2}\leqslant x\leqslant x_0\right\}, \tag{2.15}$$
$$l_{n+1}=Bl_n, \quad x_n=-\frac{x_{n-1}}{2},\ n\geqslant 1,$$

where $B = -\frac{1}{2}I$ and I is the identity matrix. Combining the first equation of system (2.14) with relations (2.15) results in the differential equation

$$x' = (-1)^n \sqrt{\frac{(-1)^{n-1}}{3\mu_0}(x_{n-1} + 2x)}$$

describing the evolution of x between the time moments t_{n-1} and t_n when the trajectory passes through the end points $(x_{n-1}, 0)$ and $(x_n, 0)$ of the arc l_n. This equation has the explicit solution

$$\sqrt{3\mu_0}\big(\sqrt{(-1)^{n-1}3x_{n-1}} - \sqrt{(-1)^{n-1}(x_{n-1} + 2x)}\big) = t - t_{n-1}$$

for $t_{n-1} \leqslant t \leqslant t_n$, $n \geqslant 1$, which in particular implies $t_n - t_{n-1} = 3\sqrt{\mu_0 x_0/2^{n-1}}$. Summing this differences over n and taking into account that $(x(t_n), y(t_n)) = (x_n, 0) \to 0$ as $n \to \infty$, we see that the trajectory reaches the zero equilibrium in finite time $T = 3\sqrt{2\mu_0 x_0}/(\sqrt{2} - 1)$, proving the backward non-uniqueness of solutions.

The uniqueness problem for the scalar equation $(Px)' = f(t, x)$ has been studied in [37], [2]. This equation can have isolated points of forward non-uniqueness, which are identified in [37] in terms of a system of equalities and inequalities for the derivatives of the function f. In natural situations, the conditions for forward uniqueness are satisfied everywhere [38], [50], [2], [11]. In this paper, we restrict the analysis of uniqueness for system (1.7) to the above discussion. A complete analysis remains an open problem. We note that Example 1 is 'exotic' in the sense that if a solution of system (2.12) does not start from the line $x = 0$ (that is, the line $f(x, y) = 0$), then the solution never reaches this line, as $x(t)$ increases if $x(t_0) > 0$ and $x(t)$ decreases if $x(t_0) < 0$. Hence, all such solutions have the forward uniqueness property.

3. Main results

3.1. Behaviour of solutions near the curve $f = 0$. As discussed in Section 2.4, for any solution of system (1.7) defined for $t \geqslant t_0$, the state $S(t)$ at a moment $t > t_0$ has a nonzero initial horizontal segment whenever $f(x(t), y(t)) > 0$, and an initial nonzero vertical segment whenever $f(x(t), y(t)) < 0$. By this reason, and due to the special role of the line $f = 0$ highlighted in the previous section, we will consider only initial data $(x(t_0), y(t_0), S(t_0)) = (x_0, y_0, S_0)$ satisfying $f(x_0, y_0) \neq 0$, where S_0 has a nonzero initial horizontal segment if $f(x_0, y_0) > 0$, and a nonzero initial vertical segment if $f(x_0, y_0) < 0$. Such data will be called admissible.

In what follows, we assume relations (2.8) at the origin $x_0 = y_0 = 0$ and the nondegeneracy condition (2.10).

Theorem 3.1. *Assume that $f_y(0,0) \neq 0$. The set of the moments t_k when a trajectory of a solution $(x(t), y(t))$ of system (1.7) intersects the line $f = 0$ away from the origin consists (if nonempty) of isolated points. Each point t_k is a local extremum point of the component $x(t)$, which is strictly monotone to the left and right of t_k. The derivative of $x(t)$ has a jump at each point t_k: the left derivative $D_-x(t_k)$ is zero, while the right derivative is defined by the formula*

$$D_+x(t_k) = \frac{\operatorname{sign}(f_y g)}{2\mu_0}\left(f_x + \sqrt{(f_x)^2 + 4\mu_0|f_y g|}\right) \tag{3.1}$$

where f_x, f_y, g are evaluated at the point $(x(t_k), y(t_k))$ and $\mu_0 = \mu(x(t_k), x(t_k))$.

According to this theorem, any trajectory has a corner point when it crosses the line $f = 0$ away from the origin. It approaches and leaves the line $f = 0$ transversally passing to the other side of the line and changing the direction at the crossing point. A trajectory always approaches the line $f = 0$ vertically; for the intersections near the origin, it leaves the line $f = 0$ almost horizontally in case $f_x(0,0) > 0$, and almost parallelly to the line $f = 0$ in case $f_x(0,0) < 0$.

Theorem 3.1 implies that a trajectory of equation (1.7) either has at most finite number of intersections with the line $f = 0$ on any finite time interval and never reaches the origin, or a trajectory reaches the zero equilibrium in finite time making infinitely many intersections with the line $f = 0$. In the latter case, the intersection moments $t_1 < t_2 < t_3 < \ldots < \infty$ converge to the moment when the trajectory reaches the origin as illustrated by the example of Subsection 2.4.

3.2. Systems with $f_x(0,0) > 0$.

Theorem 3.2. *Let $f_x(0,0) > 0$. There is a function $\varphi = \varphi(\delta)$ satisfying $0 < \varphi(\delta) < \delta$ such that if, at some moment τ, a trajectory of system (1.7) hits the line $f = 0$ at a point (x, y) with $0 < |x| < \varphi(\delta)$ for a sufficiently small δ, then the trajectory escapes the strip $|x| < \delta$. The x-component of the trajectory is strictly monotone between the moment τ and the moment $\tau_e > \tau$ when the trajectory first hits one of the lines $x = \pm\delta$ (hence, the trajectory does not intersect the line $f = 0$ for $\tau < t < \tau_e$). Moreover, there is a function $\varphi = \varphi(\delta) > 0$ satisfying $\varphi(\delta) \to 0$ as $\delta \to 0$ such that $|\mathrm{d}y/\mathrm{d}x| < \varphi(\delta)$ for $\tau < t < \tau_e$ as long as $0 < |x| < \varphi(\delta)$.*

According to this theorem, a trajectory, which hits the line $f = 0$ sufficiently close to the zero equilibrium, continues almost horizontally until it escapes some fixed vicinity of zero. Figure 3 (a) presents a numerical solution of system $(Px)' = x - y$, $y' = x + y$ satisfying the conditions of Theorem 3.2.

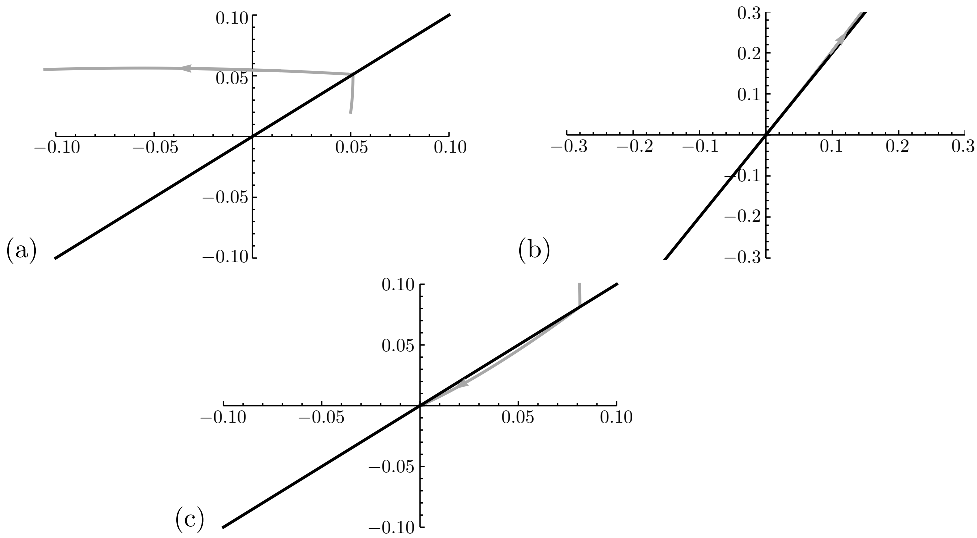

Figure 3. Numerical solution of systems (a) $(Px)' = x - y$, $y' = x + y$; (b) $(Px)' = -2x + y$, $y' = -x + y$; (c) $(Px)' = -x + y$, $y' = -2x - y$. The line with the arrow shows the trajectory of a solution. The other line is $f(x, y) = 0$. The Preisach density function is $\mu(\alpha, \beta) = 1$. The initial state of the Preisach operator is a single horizontal line connected to the edge of the strip Π for panels (a) and (c); for panel (b), it includes an initial vertical line connected to a horizontal line which goes to the edge of the strip Π.

3.3. Systems with $f_x(0,0) < 0$.

Theorem 3.3. *Let $f_x(0,0) < 0$, $j_0 < 0$ and $f_y(0,0) \neq 0$. There is a function $\varphi = \varphi(\delta)$ satisfying $0 < \varphi(\delta) < \delta$ such that if, at some moment τ, a trajectory of system (1.7) hits the line $f = 0$ at a point (x, y) with $0 < |x| < \varphi(\delta)$ for a sufficiently small δ, then the trajectory escapes the strip $|x| < \delta$. The x-component of the trajectory is strictly monotone between the moment τ and the moment $\tau_e > \tau$ when the trajectory first hits one of the lines $x = \pm\delta$ (hence, the trajectory does not intersect the line $f = 0$ for $\tau < t < \tau_e$). Moreover, there is a function $\varphi = \varphi(\delta) > 0$ satisfying $\varphi(\delta) \to 0$ as $\delta \to 0$ such that a trajectory lies in the angle $|f_x(0,0)x + f_y(0,0)y| < \varphi(\delta)|x|$ for $\tau < t < \tau_e$ whenever it hits the line $f = 0$ at a point (x, y) with $0 < |x| < \varphi(\delta)$.*

Under the conditions of this theorem, a trajectory, which hits the line $f = 0$ sufficiently close to the zero equilibrium, continues along the line $f = 0$ until it escapes some fixed vicinity of zero. Figure 3 (b) illustrates Theorem 3.3 for system $(Px)' = -2x + y$, $y' = -x + y$.

Theorem 3.4. *Let $f_x(0,0) < 0$, $j_0 > 0$ and $f_y(0,0) \neq 0$. Then any trajectory of system (1.7) that hits the line $f = 0$ sufficiently close to the zero equilibrium* *at some moment τ, converges to the zero equilibrium, but never reaches it. The x-component of the trajectory is strictly monotone for $t > \tau$ (hence, the trajectory does not intersect the line $f = 0$ for $t > \tau$). Moreover, there is a function $\varphi = \varphi(\delta) > 0$ satisfying $\varphi(\delta) \to 0$ as $\delta \to 0$ such that $|f_x(0,0)x + f_y(0,0)y| < \varphi(|x(\tau)|)|x|$ for $t > \tau$.*

As in Theorem 3.3, the assumption $f_x(0,0) < 0$ ensures that a trajectory that hits the line $f = 0$ sufficiently close to the zero equilibrium then continues along the line $f = 0$. Under the condition $j_0 > 0$ of Theorem 3.4 the trajectory moves along the line $f = 0$ towards the zero equilibrium, while under the condition $j_0 < 0$ of Theorem 3.3 the trajectory moves away from zero. Figure 3 (c) illustrates Theorem 3.4 for system $(Px)' = -x + y$, $y' = -2x - y$.

A trajectory cannot hit the line $f = 0$ exactly at the zero equilibrium point without having made a sequence of previous intersections with this line at some points $(x_k, y_k) \to (0,0)$. Indeed, as long as a trajectory does not hit the line $f = 0$, it is a solution of the smooth ordinary differential system of equations (2.11) with $L(x) > 0$ separated from zero. Such a solution cannot reach the zero equilibrium due to the uniqueness property.

The condition $f_y(0,0) \neq 0$ of Theorems 3.3, 3.4 is technical and can be omitted.

3.4. Similarity with slow-fast systems. The behaviour of trajectories of system (1.7) described in Theorems 3.2–3.4 after a trajectory hits the line $f = 0$ near the zero equilibrium is similar to that of the slow-fast system

$$\begin{aligned} \varepsilon x' &= f(x,y), \\ y' &= g(x,y) \end{aligned} \tag{3.2}$$

with $0 < \varepsilon \ll 1$. The reason for this similarity is that the factor $L(x)$ in equation (2.11) equivalent to system (1.7) is small after the trajectory intersects the line $f = 0$. Some difference is due to the fact that, when a trajectory moves away from the line $f = 0$ after having hit this line, the value of $L(x)$ increases from zero to positive values, hence it is first smaller than any ε and later it becomes larger than a sufficiently small ε. For the three examples illustrating Theorems 3.2–3.4 in the previous subsection, we replace $(Px)'$ with $\varepsilon x'$ and present trajectories of the resulting linear systems in Figure 4. We note that if a trajectory of system (1.7) approaches a neighbourhood of the zero equilibrium from a distance without hitting the line $f = 0$, then $L(x)$ is not small and therefore this part of the trajectory is not similar to trajectories of system (3.2).

3.5. Stability and effect of small impulse perturbations. Now, we use Theorems 3.2–3.4 to analyze stability of the zero equilibrium of system (1.7). In order

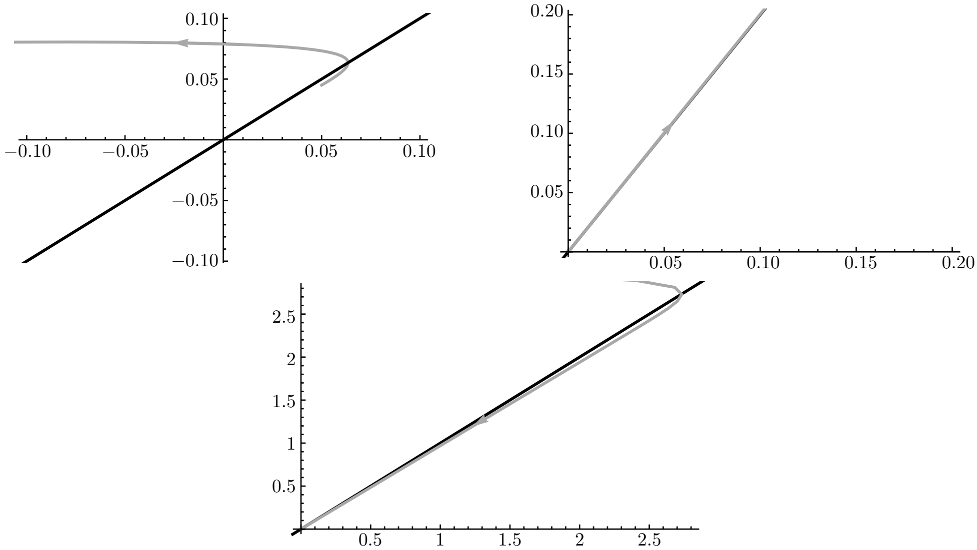

Figure 4. A trajectory of the slow-fast ordinary differential system $\varepsilon x' = x - y$, $y' = x + y$ (left) is similar to the trajectory of system $(Px)' = x - y$, $y' = x + y$ shown in Figure 3 (a) after the trajectories cross the line $x - y = 0$. Trajectories of the system $\varepsilon x' = -2x + y$, $y' = -x + y$ (center) and system $\varepsilon x' = -x + y$, $y' = -2x - y$ (right) are similar to those shown in Figures 3 (b) and 3 (c), respectively. The initial conditions used for these solutions are the same as those used in the corresponding system with the Preisach operator.

to simplify the analysis, we restrict ourselves to the class Σ_ν, $\nu > 0$, of initial states S_0 of the Preisach operator, which satisfy the following properties:

A staircase $S_0 \in \Sigma_\nu$ either consists of one segment; or, it consists of two segments and the length of the initial segment is larger than $d - \nu$ where d is the width of the stripe Π on the Preisach plane; or, the length of the initial segment and the length of the second segment is larger than ν, see Figure 5.

Definition. The zero equilibrium is *ν-asymptotically stable* if for any $\varepsilon > 0$ there is a $\delta > 0$ such that the relations $|x_0| + |y_0| < \delta$ and $S_0 \in \Sigma_\nu$ ensure that a solution of system (1.7) with the initial data $x(t_0) = x_0$, $y(t_0) = y_0$ and S_0 satisfies $|x(t)| + |y(t)| < \varepsilon$ for all $t > t_0$ and $x(t), y(t) \to 0$ as $t \to \infty$.

Definition. The zero equilibrium is *ν-partially asymptotically stable* if (a) for any $\varepsilon > 0$ there is an open ball in the product of the (x, y) phase plane and the set Σ_ν of the state space of the Preisach operator such that any solution of system (1.7) with initial data from this ball satisfies $|x(t)| + |y(t)| < \varepsilon$ for all $t > t_0$ and $x(t), y(t) \to 0$ as $t \to \infty$; and, at the same time, (b) there is an $\varepsilon > 0$ such that for every $\delta > 0$ there is an open ball in the product of the disc $|x| + |y| < \delta$ and the

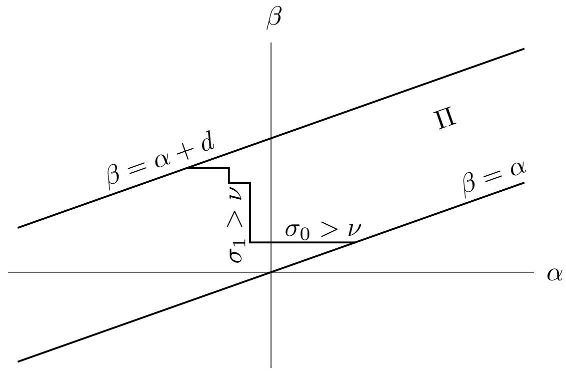

Figure 5. States S_0 of the Preisach operator from the set Σ_ν.

set Σ_ν of states of the Preisach operator such that any solution of system (1.7) with initial data from this ball satisfies $|x(t)| + |y(t)| \geqslant \varepsilon$ at some moment $t > t_0$.

Definition. The zero equilibrium is *ν-completely unstable* if there is an $\varepsilon > 0$ such that, given any sufficiently small x_0, any initial state $S_0 \in \Sigma_\nu$ of the Preisach operator and any sufficiently small y_0 (except for one value of y_0 for every given x_0 and S_0), if $x(t_0) = x_0$, $y(t_0) = y_0$, $S(t_0) = S_0$ are admissible initial data and $|x_0| + |y_0| > 0$, then the solution of system (1.7) with these initial data satisfies $|x(t)| + |y(t)| \geqslant \varepsilon$ at some moment $t > t_0$.

In the last definition, we exclude a small set of initial data (namely, one value of y_0 for each given x_0 and S_0), as a ν-completely unstable equilibrium of system (1.7) is, typically, of the saddle type (see the proof of Theorem 3.5 below). Trajectories starting from this small set can converge to the equilibrium.

Define

$$L_{\max} = \max\left\{\int_0^d \mu(\alpha,0)\,\mathrm{d}\alpha, \int_0^d \mu(0,\beta)\,\mathrm{d}\beta\right\},$$
$$L_{\min}^\nu = \min\left\{\int_0^\nu \mu(\alpha,0)\,\mathrm{d}\alpha, \int_0^\nu \mu(0,\beta)\,\mathrm{d}\beta\right\}.$$

Theorem 3.5. *Assume $f_x(0,0) \neq 0$, $f_y(0,0) \neq 0$. The following statements hold for any $\nu > 0$.*

(i) *If $f_x(0,0) < 0$, $j_0 > 0$ and*

$$f_x(0,0) + Lg_y(0,0) < 2\sqrt{j_0 L} \quad \textit{for all} \quad L_{\min}^\nu \leqslant L \leqslant L_{\max}, \tag{3.3}$$

then the zero equilibrium is ν-asymptotically stable.

(ii) *If* $f_x(0,0) < 0$, $j_0 > 0$ *and*

$$f_x(0,0) + \widetilde{L} g_y(0,0) > 2\sqrt{j_0 \widetilde{L}} \quad \textit{for some} \quad \widetilde{L} \in (L^{\nu}_{\min}, L_{\max}), \tag{3.4}$$

then the zero equilibrium is ν*-partially asymptotically stable.*

(iii) *If* $f_x(0,0) > 0$, $j_0 > 0$ *and*

$$f_x(0,0) + \widetilde{L} g_y(0,0) < -2\sqrt{j_0 \widetilde{L}} \quad \textit{for some} \quad \widetilde{L} \in (L^{\nu}_{\min}, L_{\max}), \tag{3.5}$$

then the zero equilibrium is ν*-partially asymptotically stable.*

(iv) *If* $f_x(0,0) > 0$, $j_0 > 0$ *and*

$$f_x(0,0) + L g_y(0,0) > -2\sqrt{j_0 L} \quad \textit{for all} \quad L^{\nu}_{\min} \leqslant L \leqslant L_{\max}, \tag{3.6}$$

then the zero equilibrium is ν*-completely unstable.*

(v) *If* $j_0 < 0$, *then the zero equilibrium is* ν*-completely unstable.*

Note that stability of the zero equilibrium of the slow-fast system (3.2) is determined by the signs of $f_x(0,0)$ and j_0 for all sufficiently small $\varepsilon > 0$: the equilibrium is a stable node if $f_x(0,0) < 0$, $j_0 > 0$, an unstable node if $f_x(0,0) > 0$, $j_0 > 0$, and a saddle if $j_0 < 0$ (cf. cases (i), (iv), (v) of Theorem 3.5).

3.6. Excitability. A system which rests at, or near, an equilibrium state in the absence of external perturbations is called *excitable* if a relatively small and short perturbation can cause the system to make a large excursion in the phase space before returning back to the equilibrium. A classical mechanism leading to the excitability of ordinary differential systems is the saddle-node homoclinic bifurcation, which creates a pair of equilibria connected by a short and a long heteroclinic orbits (see e.g. [35], [29]). Perturbations which instantaneously move a point in the phase space within the basin of attraction of the unstable node are followed by the convergence back to the node along the short homoclinic orbit. Hence, they have little effect on dynamics. However, if a fluctuation moves the state from a vicinity of the stable node beyond the stable manifold of the saddle equilibrium, then the trajectory returns to the node along the long homoclinic orbit, thus resulting in a strong response to a relatively small perturbation. This dynamics typically manifests itself by a large pulse in the time trace of the phase variables. The distance between the saddle and the node defines the size of perturbations which are capable of causing the pulse response.

Partially stable equilibria of system (1.7) seem to provide a possibility of a more robust type of excitability. If an equilibrium is partially stable, then coupling of the local dynamics near the equilibrium with global dynamics can make trajectories that leave a small vicinity of the equilibrium to come back after having made a large excursion in the phase space, which is a premise for an excitable response to small perturbations. Indeed, assume that, conditions of case (iii) of Theorem 3.5 are satisfied and therefore the zero equilibrium is partially stable. Consider an initial point (x_0, y_0) in the domain $f(x,y) > 0$, $x < 0$ and an admissible initial Preisach state $\widetilde{S}_0 \in \Sigma_\nu$, which has a horizontal initial segment with $L_{\widetilde{S}_0}(x_0) = \widetilde{L}$ satisfying (3.5). The trajectory $(x(t), y(t))$ of system (1.7) starting from this point is a solution of the ordinary differential system $L_{\widetilde{S}_0}(x)x' = f(x,y)$, $y' = g(x,y)$ as long as it does not cross the line $f = 0$. Due to (3.5), the zero equilibrium is a stable node of this system with eigenvalues $\lambda_2 < \lambda_1 < 0$. Choosing an eigenvector e_1 corresponding to the eigenvalue λ_1 in such a way that its x-component is negative, it is straightforward to see that there is an angle $\mathcal{A} \subset \{(x,y)\colon\ a_1x + b_1y \leqslant 0, a_2x + b_2y \leqslant 0,\ x \leqslant 0\}$ with the vertex at zero and a disc U centered at zero such that (a) $\mathcal{A}$ contains the ray re_1, $r > 0$ in its interior; (b) the interior of the intersection $\mathcal{A} \cap U$ is contained in the domain $f(x,y) > 0$, $x < 0$; and, (c) if (x_0, y_0) belongs to $\mathcal{A} \cap U$, then the trajectory of the system $L_{\widetilde{S}_0}(x)x' = f(x,y)$, $y' = g(x,y)$ starting from the point (x_0, y_0) converges to zero within the angle $\mathcal{A}$, asymptotically approaching the ray re_1. Hence, the same property (c) is true for all the trajectories of system (1.7) with initial data $(x_0, y_0) \in \mathcal{A} \cap U$ and any admissible initial state with $S_0 \in \Sigma_\nu$ sufficiently close to $\widetilde{S}_0$, i.e., all such trajectories converge to zero within the angle $\mathcal{A}$.

Now assume that a small instant perturbation affects the x-component of such a solution at a moment τ, namely x instantly changes to $x - \varepsilon$ where $\varepsilon > 0$. We assume that the state of the Preisach operator changes at the same instant appropriately, acquiring a small vertical segment of length ε, which corresponds to a monotonic change of the input from the value x to the value $x - \varepsilon$. As $f(x(t), y(t)) > 0$ for $t < \tau$, the x-component of the solution was increasing prior to the perturbation, hence $S(\tau) \in \Sigma_\varepsilon$. If the perturbation happens at a large moment τ, then x is close to zero and therefore the perturbation moves the point (x,y) across the line $f = 0$ to the domain $f < 0$, $x < -\varepsilon$, hence x decreases after the moment τ. Moreover, an argument similar to that we use in the proof of Theorem 3.2 below shows that after the moment τ the trajectory is almost horizontal and its x-component decreases until the trajectory crosses the line $x = -\delta$ through a segment $R_\delta = \{x = -\delta, -a(\delta) \leqslant y \leqslant a(\delta)\}$, where $0 < \delta < \delta_0$ is independent of the value of ε which can be arbitrarily small, and $a(\delta) \to 0+$ as $\delta \to 0$.

Now, if this local dynamics couples with global dynamics which returns the trajectory from the segment R_δ to the arc $\mathcal{A} \cap \partial U$, where ∂U is the boundary of the disc U, and, simultaneously, returns the state of the Preisach nonlinearity to a state $S \in \Sigma_\nu$ which has approximately the same initial segment as the state $\widetilde{S}_0$, then this combination of dynamics ensures the excitability.

An explicit rigorous example of such a coupling of local and global dynamics is an open problem. Note that the suggested excitable dynamics are robust with respect to small perturbations of the system. This robustness contrasts to the excitability scenario in ordinary differential equations, where a small variation of system parameters can eliminate a pair of close equilibria connected by two heteroclinic orbits via the saddle-node homoclinic bifurcation, thus eliminating the excitability property. A partially stable equilibrium of system (1.7) is similar to a saddle-node equilibrium of an ordinary differential equation in that, in both systems, there are many trajectories which converge to the equilibrium and, simultaneously, many trajectories which diverge from it. However, while the partially stable equilibrium is robust, the saddle-node is not. Trajectories which leave a small neighbourhood of a partially stable equilibrium of system (1.7) and then are caught into the basin of attraction of the same equilibrium due to global dynamics can also be compared to trajectories of an ordinary differential system near a homoclinic loop connecting the unstable and stable manifolds of a saddle equilibrium. Again, we suggest that such trajectories of system (1.7) are robust, while the homoclinic loop will, generically, be destroyed by an arbitrarily small perturbation of the ordinary differential system via the homoclinic bifurcation.

3.7. Solutions that do not hit the line $f = 0$. Theorems 3.2–3.4 discuss the behaviour of trajectories that hit the line $f = 0$ near the zero equilibrium. As we have seen in the previous subsection, there might be other trajectories, which converge to the zero equilibrium without hitting the line $f = 0$ (see also the proof of Theorem 3.5 below). After some moment τ, such trajectories satisfy an ordinary differential system (2.11) and converge to zero along the less stable direction of the stable zero node of system (2.11). However, in case of a partially stable equilibrium of system (1.7), such trajectories are unstable to small perturbations which can push them to the domain where the equilibrium of system (1.7) repels. In particular, as discussed above, this local dynamics can be a premise for the excitability.

3.8. Examples and open problems. The LCR circuit system (1.5) with $L = 0$ is an example of system (1.7). It satisfies condition (3.3) of Theorem 3.5, hence the zero equilibrium $j = 0$, $u = 0$ of this system is ν-asymptotically stable, as expected.

Let us consider another example of a stable equilibrium coming from hydrology. The following lumped model of a water flow through a slab of soil has been derived in [47], [48] by combining Darcy's law with the hysteretic constitutive relationship between the moisture content and the water pressure in the soil, and averaging out the spatial variation of the variables:

$$u' = k(a(t) - x), \quad u(t) = (Px)(t). \tag{3.7}$$

Here u is the amount of water in the soil column; x is the pressure (or, equivalently, the so-called matric potential) in the center of the soil column; a is the pressure on the surface of the soil controlled by the conditions in the atmosphere such as precipitation and humidity. The first equation is the balance equation stating that the rate of change of the water content equals the water flux from the surface into the soil slab, which is proportional to the difference of pressures on the surface and in the soil. The second equation is the constitutive hysteretic relationship between u and x defined by the properties of the porous media of the soil and modelled by the Preisach operator P. This model and its extensions with multiple flows from and to the soil slab have been studied in [37], [2], [38], [8], [26], [46], [53], [49]. In particular, the Preisach operator density function has been identified for different types of soils on the basis of the measured constitutive relationship in [25]; the model has been fitted to experimental rainfall and soil water content data in [2], [8].

Let us consider a similar model with two layers of two different soils. The upper layer is the same as above. In the lower layer, we assume simply the linear constitutive relationship between the water content and the pressure. The resulting system

$$u' = k_1(a - x) + k_2(y - x), \quad v' = k_2(x - y), \quad u(t) = (Px)(t), \quad v = Cy$$

has the form (1.7), where x, y are the pressures in the lower and upper soil layers, respectively; a is the pressure on the surface; u and v are the water contents in the upper and lower soil layers; k_1 and k_2 are hydrolic conductivities of those. If a is constant, then the equilibrium is achieved for $x = y = a$. The system satisfies the conditions of part (i) of Theorem 3.5, hence the equilibrium is ν-asymptotically stable. In hydrological applications it is natural to assume that the hydrolic conductivities depend on the pressure, $k_1 = k_1(x)$, $k_2 = k_2(y)$, and that the constitutive relationship is nonlinear, $v = C(y)$. One can apply Theorem 3.5 in this context too.

Several examples of models of population dynamics in ecology, epidemiology and economics lead to extensions of system (1.7). As one illustration, let us consider the following Predator-Prey system, where prey can migrate between two patches of habitat, a free patch and a refuge. The free patch is characterized by certain uniform growth rate b of the prey and attack rate a by the predator. The prey growth rate and the attack rate in the refuge are for simplicity assumed to be zero. We further assume that the heterogeneous refuge consists of many cells where each cell is characterized by two thresholds α and β with $\alpha < \beta$. A refuge cell gets filled with prey when the density x of predator exceeds the higher threshold value β; the cell gets emptied when the predator density x decreases below the lower threshold[4] α.

[4] The difference between the threshold values can be caused by herding behaviour of the prey.

This behaviour is modelled by the non-ideal relay (2.1), which switches between the "filled" state 1 and the "empty" state 0 in response to the variations of the predator density $x(t)$. In the continuous limit, assuming the density of prey $\mu(\alpha,\beta)$ in the refuge cell with thresholds α,β when it is filled, we obtain that the total number of prey in the refuge is given by the integral (2.3). That is, the Preisach operator maps the time series of x to the time series of the number of prey in the refuge. Therefore, the total number of prey is $y+Px$ where y is the number of prey in the free patch. Assuming that the transitions of prey between the free and refuge patches are much faster than the population processes, we arrive at the predator-prey system

$$\begin{aligned} x' &= -dx - cx^2 + eaxy, \\ y' + (Px)' &= by - axy, \end{aligned} \tag{3.8}$$

where d is the death rate of the predator, c is the competition rate coefficient and e is the predator efficiency. This system does not have the form (1.7), hence a modification of Theorem 3.5 is needed to analyse its stability. Numerical simulations give an evidence that the unique positive equilibrium $x_*=b/a$, $y_*=(ad+bc)/(a^2e)$ of (3.8) is globally stable. A rigorous analysis is beyond the scope of this paper.

A similar modelling approach was used in [51], [52] to formulate a Susceptible-Infected-Recovered epidemiological model where people can switch from a riskier to a safer mode of behaviour in the face of epidemics and switch back when the risk of contagion decreases. The resulting model is more complex than (1.7) or (3.8) in that it contains both the Preisach operator Px and the time derivative $(Px)'$. Such models are typically characterized by multiple equilibrium points forming connected sets or branches. A rigorous analysis of stability of such equilibrium sets, to the best of our knowledge, has not been attempted yet. Moreover, a similar set of ideas has been applied in the context of models of economics and finance in order to explain multiplicity of equilibria, persistent memory of shocks and other stylized features observed in economic processes. For example, a Supply-Demand model of this type was developed in [17]; further material related to the role of hysteresis in economics can be found in [28], [12], [13], [14], [15], [16]. A single equation (3.7) was considered in [11] as a prototype model of supply driven by investment or, in a broader context, a model of economic flows related to large ensembles of exchange operations exhibiting hysteresis. A stochastic counterpart of equation (3.7) was used to model price dynamics in a market with hysteretic agents [45]. Global stability of a periodic solution of equation (3.7) driven by a non-stationary periodic input $a(t)$ was shown in [38]. In case of a stationary input $a(t)\equiv a$, this global result agrees with Theorem 3.5 as the decoupled system $(Px)'=k(a-x)$, $y'=-y$ satisfies the conditions of part (i) of Theorem 3.5, which ensure the ν-asymptotic stability of the equilibrium.

4.1. Proof of Theorem 3.1. Suppose a trajectory $(x(t), y(t))$ hits the line $f = 0$ at a moment $t = \tau$ at a point $(x_0, y_0) \neq 0$ close to the origin. Assume

$$f_y(x_0, y_0)g(x_0, y_0) > 0 \tag{4.1}$$

(the other case $f_y(x_0, y_0)g(x_0, y_0) < 0$ can be considered similarly). Consider

$$\frac{\mathrm{d}f(x(t), y(t))}{\mathrm{d}t} = f_x(x(t), y(t))x'(t) + f_y(x(t), y(t))g(x(t), y(t)). \tag{4.2}$$

As on some time interval $\tau - \delta < t < \tau$ the component $x(t)$ is strictly monotone, x' is defined and satisfies $|x'(t)| < k|f(x(t), y(t))|$ with some $k > 0$ almost everywhere on $\tau - \delta/2 < t < \tau$. This inequality combined with (4.1), (4.2) and $f(x_0, y_0) = 0$ implies that $f(x(t), y(t))$ strictly increases on a sufficiently small time interval $(\tau - \varepsilon, \tau]$, hence $f(x_0, y_0) = 0$ implies $f(x(t), y(t)) < 0$ for $t \in (\tau - \varepsilon, \tau)$. If we assume that $f(x(t), y(t)) \leqslant 0$ also on some time interval $(\tau, \tau + \delta_1)$ after the moment τ, then, similarly, $\mathrm{d}f(x(t), y(t))/\mathrm{d}t > 0$ almost everywhere on a sufficiently small time interval $(\tau - \varepsilon, \tau + \varepsilon)$, hence $f(x(t), y(t)) > 0$ for $t > \tau$, i.e., we arrive at a contradiction. Therefore, there are moments $\theta > \tau$ arbitrarily close to τ such that $f(x(\theta), y(\theta)) > 0$. Moreover, if θ is such a moment and if we assume that $f(x(t), y(t)) > 0$ on a time interval $[\theta, \theta_1)$ with $f(x(\theta_1), y(\theta_1)) = 0$, while the trajectory does not leave some sufficiently small neighbourhood of the point (x_0, y_0) during this time interval, then (4.2) implies that $\mathrm{d}f(x(t), y(t))/\mathrm{d}t > 0$ almost everywhere on some interval $t \in (\theta_1 - \delta, \theta_1) \subset (\theta, \theta_1)$, which implies $f(x(t), y(t)) < f(x(\theta_1), y(\theta_1)) = 0$ on $(\theta_1 - \delta, \theta_1)$ and thus makes a contradiction with the assumption $f(x(t), y(t)) > 0$ on the whole interval $[\theta, \theta_1)$. This contradiction shows that if $f(x(\theta), y(\theta)) > 0$ for a $\theta > \tau$ sufficiently close to τ, then $f(x(t), y(t)) > 0$ for $t > \theta$ as long as the trajectory is sufficiently close to (x_0, y_0). As such θ exist arbitrarily close to τ, we conclude that $f(x(t), y(t)) > 0$ on some time interval $(\tau, \tau + \varepsilon)$.

The relations $f(x(t), y(t)) < 0$ on $t \in (\tau - \varepsilon, \tau)$ and $f(x(t), y(t)) > 0$ on $(\tau, \tau + \varepsilon)$ imply that the intersection point τ of the trajectory with the line $f = 0$ is isolated and that τ is a minimum point of the component $x(t)$, which strictly decreases to the left of τ and strictly increases to the right of τ.

It remains to prove formulas $D_{-}x(\tau) = 0$ and (3.1) at $t_k = \tau$. The first follows from the relations $f(x_0, y_0) = 0$, $L(x(t)) > 0$ where $L(x)$ is the coefficient (2.7) in the ordinary differential system (2.11) which is equivalent to system (1.7) on the time interval $\tau - \varepsilon < t < \tau$. To prove the second formula, note that $x(t)$ is absolutely continuous for $t \geqslant \tau$. (Indeed, consider the function $z(x) = \int_{x(\tau)}^{x} L(s)\,\mathrm{d}s$;

the first equation of system (2.11) implies $z' = f(x(z), y)$, hence $z(t)$ is continuously differentiable for $t \geqslant \tau$ and $x(t) = x(z(t))$ is continuously differentiable for $t > \tau$ and absolutely continuous for $t \geqslant \tau$.) Therefore, $x(t) - x(\tau) = \int_\tau^t x'(\theta)\,\mathrm{d}\theta$. Set $\Delta x = x(t) - x(\tau)$, $\Delta y = y(t) - y(\tau)$, $\Delta t = t - \tau$. Assume $\Delta x \geqslant k\Delta t$ with $k > 0$, then relations

$$x' = \frac{1}{\mu_0 + o(1)}\Big(f_x + \frac{f_y \Delta y}{\Delta x} + o(1)\frac{|\Delta y| + \Delta x}{\Delta x}\Big) \quad \text{as} \quad \Delta t \to 0+$$

and $\Delta y = g\Delta t + o(\Delta t)$ with $f_x = f_x(x_0, y_0)$, $f_y = f_y(x_0, y_0)$, $g = g(x_0, y_0)$ imply

$$x' = \frac{1}{\mu_0}\Big(f_x + \frac{f_y g}{k} + o(1)\Big);$$

here $o(1)$ is a small quantity which vanishes at the point (x_0, y_0). The expression on the right hand side is less than k for sufficiently small Δt provided that $k > k_+$, where k_+ is the positive root of the quadratic equation $\mu_0 k^2 - f_x k - f_y g = 0$. Hence,

$$\Delta x(t) \geqslant k\Delta t > k_+\Delta t \quad \Rightarrow \quad x'(t) < k \tag{4.3}$$

for $\Delta t > 0$ small enough. Similarly,

$$\Delta x(t) \leqslant k\Delta t < k_+\Delta t \quad \Rightarrow \quad x'(t) > k. \tag{4.4}$$

If $\Delta x(t) > k\Delta t > k_+\Delta t$ and $t_1 \in [\tau, t]$ is the latest moment such that $\Delta x(t_1) = k\Delta t_1$, then integrating the inequality $x'(t) < k$ over the segment $[t_1, t]$, we obtain $x(t) - x(t_1) < k(t - t_1)$ which contradicts $x(t) - x(t_1) = \Delta x(t) - \Delta x(t_1) > k\Delta t - k\Delta t_1 = k(t - t_1)$. Hence, given any $k > k_+$, (4.3) implies $\Delta x(t) \leqslant k\Delta t$ for all sufficiently small $\Delta t > 0$. Similarly, given a $k < k_+$, (4.4) implies $\Delta x(t) \geqslant k\Delta t$. Hence, $D_+x(\tau) = k_+$ and the proof is complete. □

4.2. Proof of Theorem 3.2. We use the notation of the previous subsection. Given any small $\varepsilon, \nu > 0$, we can choose a $\delta > 0$ such that $|g(x, y)| < \varepsilon$ in the rectangle $K = \{|x| \leqslant \delta, |y| \leqslant \delta + 2\delta\nu\}$. Assume that a trajectory $(x(t), y(t))$ hits the line $f = 0$ at a moment $t = \tau$ at a point $(x_0, y_0) \neq 0$ inside the rectangle $|x| < \delta, |y| < \delta$. To be definite, assume $x(t)$ strictly increases on an interval $[\tau, \tau_1)$ (the case when $x(t)$ strictly decreases after the moment τ is similar). According to (3.1),

$$D_+x(\tau) = f_x(0,0)/\mu_0 + o(1) > 0 \quad \text{as} \quad \delta \to 0,$$

while $|y'(\tau)| = |g(x_0, y_0)| < \varepsilon$, hence choosing $\nu = 2\varepsilon\mu_0/f_x(0,0)$ and making $\delta > 0$ sufficiently small we ensure that the trajectory enters the angle $A = \{|y - y_0| <$

$\nu(x-x_0)\}$. Also, the smallness of ν ensures that the set $A\cap K$, which is at the same time the intersection of the angle A with the vertical strip $|x|\leqslant\delta$, does not intersect the line $f=0$. Hence, as long as the trajectory belongs to $A\cap K$, the function x increases and satisfies

$$\Delta x\mu x' = L(x)x' = f(x(t),y(t)) = f_x\Delta x + f_y\Delta y \tag{4.5}$$

where f_x, f_y are evaluated at some intermediate points in A and $\mu(x,\xi)$ is evaluated at an intermediate point of the segment $|\xi|\leqslant\delta$. Therefore, taking into account that $|\Delta y/\Delta x|<\nu$ due to $(x,y)\in A$, we have

$$x' = \frac{f_x(0,0)}{\mu_0} + \frac{f_y(0,0)\Delta y}{\mu_0\Delta x} + o(1) > \frac{f_x(0,0)}{\mu_0} - \frac{\nu|f_y(0,0)|}{\mu_0} + o(1) \tag{4.6}$$

with the small term vanishing as $\delta\to 0$. As $\nu > \varepsilon\mu_0/(f_x(0,0)-\nu|f_y(0,0)|)$ for small ε, relation (4.6) combined with $|y'|<\varepsilon$ for $(x,y)\in K$ implies $|\mathrm{d}y/\mathrm{d}x|<\nu$. Thus, $|\mathrm{d}y/\mathrm{d}x|<\nu$ as long as the trajectory is inside the intersection of A with the vertical strip $|x|\leqslant\delta$ and we conclude that the trajectory is included in A until it hits the line $x=\delta$, which proves the theorem. □

4.3. Proof of Theorem 3.3. Let us use the notation of the previous subsection, but assume that $f_x(0,0)<0$, $j_0<0$. To be definite, assume again that $x(t)$ strictly increases on some interval $[\tau,\tau_1)$ after the trajectory $(x(t),y(t))$ hits the line $f=0$ at a point (x_0,y_0) at the moment τ, i.e., $f_y(x_0,y_0)g(x_0,y_0)>0$ in formula (3.1) and, by continuity, $f_y(0,0)g(x_0,y_0)>0$. Relations $f(x_0,y_0)=f(0,0)=g(0,0)=0$ imply $f_x(0,0)x_0+f_y(0,0)y_0=o(x_0)$ and

$$g(x_0,y_0) = g_x(0,0)x_0 + g_y(0,0)y_0 + o(x_0) = -\frac{j_0x_0}{f_y(0,0)} + o(x_0), \tag{4.7}$$

hence from $f_y(0,0)g(x_0,y_0)>0$, $j_0<0$ it follows that $x_0>0$. Thus, the component $x(t)$ of the trajectory is positive and increasing on a time interval $[\tau,\tau_1)$ after the moment τ. According to Theorem 3.1, $x(t)$ will be increasing and positive as long as the trajectory does not intersect the line $f=0$ and does not leave some fixed neighbourhood U_0 of the origin. Furthermore, Theorem 3.1 implies that any trajectory crossing the line $f=0$ in the half-plane $x>0$ close to the origin must approach this line vertically and from the same direction (from below if $-j_0/f_y(0,0)>0$ and hence relations $x>0$, $f(x,y)=0$ imply $y'=g(x,y)>0$ for small x, and from above if $-j_0/f_y(0,0)<0$ and hence the relations $x>0$, $f(x,y)=0$ imply $g(x,y)<0$). Since the trajectory we consider has crossed the line $f=0$ at the moment τ, we conclude that it will not cross this line again in U_0 after the moment τ. Hence $x(t)$ is positive and increasing for $t \in [\tau, \tau_u]$ where τ_u is the first moment when the trajectory reaches the boundary of U_0. As $x(t)$ increases, the pair $(x(t), y(t))$ for $\tau + \varepsilon \leqslant t \leqslant \tau_u$ is a solution of ordinary differential system (2.11) with an equilibrium at the origin, which is unique in U_0, hence the trajectory leaves U_0 in finite time, i.e., $\tau_u < \infty$.

It remains to prove the relation $|f_x(0,0)x(t)+f_y(0,0)y(t)| = o(1)|x(t)|$ for $t \in [\tau, \tau_e]$ as $\delta \to 0$, which also implies $\tau_e < \tau_u$, i.e., the trajectory hits the line $x = \delta$ before it leaves U_0. In order to do this, given a sufficiently small $\nu > 0$, consider the domain

$$\bar{A}_\delta = \Big\{(x,y)\colon\ f(x,y) \geqslant 0,\ \sigma\Big(\Delta y + \frac{f_x(x_0,y_0)}{f_y(x_0,y_0)}\Delta x\Big) \leqslant \nu\Delta x,\ x_0 \leqslant x \leqslant \delta\Big\}$$

where $x_0 < \delta$, $\Delta x = x - x_0$, $\Delta y = y - y_0$, and $\sigma = \operatorname{sign} f_y(0,0)$. Relations (3.1) and $f_x(x_0,y_0) < 0$ imply $D_+x(\tau) = -f_y(x_0,y_0)g(x_0,y_0)/f_x(x_0,y_0) + o(g(x_0,y_0))$, while $y'(\tau) = g(x_0,y_0)$, hence the right derivative $(\mathrm{d}y/\mathrm{d}x)_+$ at the point (x_0,y_0) equals

$$\Big(\frac{\mathrm{d}y}{\mathrm{d}x}\Big)_+ = -\frac{f_x(x_0,y_0)}{f_y(x_0,y_0)} + o(1)$$

with $o(1)$ vanishing at the origin. Combining this relation with the fact that $\sigma y(t)$ increases in a neighbourhood of the point τ, we see that the trajectory $(x(t), y(t))$ enters the domain $\bar{A}_\delta$ through its vertex (x_0,y_0) at the moment τ and remains in the interior of $\bar{A}_\delta$ for all $t > \tau$ sufficiently close to τ. Note that $(x(t), y(t))$ is continuously differentiable for $\tau < t < \tau_u$, since it is a solution of ordinary differential system (2.11) on each time interval $\tau < \tau + \varepsilon \leqslant t < \tau_u$.

As we have seen, the trajectory $(x(t), y(t))$ cannot leave $\bar{A}_\delta$ through the line $f = 0$. Relations (4.5) imply

$$\frac{\mathrm{d}y}{\mathrm{d}x} = \frac{y'}{x'} = \frac{\mu(x_1,y_1)g(x,y)}{f_x(x_2,y_2) + f_y(x_3,y_3)\Delta y/\Delta x}$$

with some $(x_i, y_i) \in U_0$. Hence, on the line l which is a part of the boundary of $\bar{A}_\delta$ and which is defined by $\sigma(\Delta y + f_x(x_0,y_0)\Delta x/f_y(x_0,y_0)) = \nu\Delta x$, we have

$$\frac{\mathrm{d}y}{\mathrm{d}x} = \frac{\mu(x_1,y_1)g(x,y)}{f_x(x_2,y_2) + f_y(x_3,y_3)(-f_x(x_0,y_0)/f_y(x_0,y_0) + \sigma\nu)} = o(1)$$

where $o(1)$ vanishes as the diameter of U_0 tends to zero for a constant $\nu > 0$. Noting that for $\sigma > 0$ the line l has a positive slope and bounds the domain $\bar{A}_\delta$ from above, while for $\sigma < 0$ the line l has a negative slope and bounds $\bar{A}_\delta$ from below, we see that the trajectory cannot leave the domain $\bar{A}_\delta$ through the line l if $\delta > 0$ is sufficiently small due to the relation $\mathrm{d}y/\mathrm{d}x = o(1)$, $\delta \to 0$ on l. Hence, the trajectory leaves $\bar{A}_\delta$ through the line $x = \delta$. Finally, $\bar{A}_\delta \subset \{(x,y)\colon\ |y + f_x(0,0)x/f_y(0,0)| \leqslant 2\nu|x|,\ x \geqslant 0\}$ for small $\delta > 0$, which completes the proof. $\square$

4.4. Proof of Theorem 3.4. To be definite, assume again that the component $x(t)$ strictly increases on some interval $[\tau, \tau_1]$ after a trajectory $(x(t), y(t))$ hits the line $f = 0$ at a point (x_0, y_0) at the moment τ, i.e., $f_y(x_0, y_0)g(x_0, y_0) > 0$. Under the conditions of Theorem 3.4, $j_0 > 0$, hence relations (4.7) imply $x_0 < 0$. Using the same argument as in the proof of Theorem 3.3, we see from formula (4.7) that any trajectory crossing the line $f = 0$ in the half-plane $x < 0$ close to the origin must approach this line vertically and from the same direction (from below if $-j_0/f_y(0,0) < 0$ and from above if $-j_0/f_y(0,0) > 0$). Therefore the trajectory we consider does not cross the line $f = 0$ after the moment τ as long as the trajectory does not leave the open left half-plane $x < 0$ and, furthermore, $x(t)$ increases all the time the trajectory is in this half-plane. To complete the proof, let us show that, given any small $\delta > 0$, the trajectory does not cross the line $l_\delta = \{(x, y)\colon\ y = ((-f_x(0,0) - \delta)/f_y(0,0))x,\ x < 0\}$ if $|x_0|$ is sufficiently small, and hence the trajectory converges to the zero equilibrium in the angle $\mathcal{A}_\delta$ between the lines $f = 0$ and l_δ. Indeed, the derivative $\mathrm{d}y/\mathrm{d}x$ on the line l_δ for $t > \tau$ is

$$\frac{\mathrm{d}y}{\mathrm{d}x} = L(x)\frac{g_x(0,0)x + g_y(0,0)((-f_x(0,0) - \delta)/f_y(0,0))x + o(x)}{f_x(0,0)x + f_y(0,0)((-f_x(0,0) - \delta)/f_y(0,0))x + o(x)}$$

with $x_0 < x < 0$ and $L(x) = \mu(0,0)x_0 + o(x_0)$, hence

$$\frac{\mathrm{d}y}{\mathrm{d}x} = \frac{\mu(0,0)(-j_0 - g_y(0,0)\delta)}{-f_y(0,0)\delta}\, x_0 + o(x_0).$$

If $|x_0|$ is sufficiently small, then the absolute value of the slope $\mathrm{d}y/\mathrm{d}x$ is less than the absolute value of the slope of the line l_δ and hence the trajectory cannot leave the angle $\mathcal{A}_\delta$ through this line. Finally, the fact that $x(t)$ increases implies that $(x(t), y(t))$ for $t \geqslant \tau_1$ is a solution of ordinary differential system (2.11) with a smooth right-hand side, which has an isolated equilibrium at the origin, therefore the trajectory converges to the zero equilibrium but never reaches it. $\square$

4.5. Proof of Theorem 3.5. Consider a trajectory of system (1.7) with small initial data $x(t_0) = x_0,\ y(t_0) = y_0$ such that $f(x_0, y_0) \neq 0$ and $S_0 \in \Sigma_\nu$. Recall that as long as the trajectory does not hit the line $f = 0$, it is a solution of the ordinary differential system

$$L_{S_0}(x)x' = f(x, y), \quad y' = g(x, y) \tag{4.8}$$

where $L_{S_0}(x)$ is a positive smooth function of x as long as x remains small; this function is separated from zero uniformly with respect to $S_0 \in \Sigma_\nu$ and continuously depends on S_0. Eigenvalues of the linearization of system (4.8) at zero are

$$\lambda_{1,2} = \frac{1}{2L}\left(f_x(0,0) + Lg_y(0,0) \pm \sqrt{\left(f_x(0,0) + Lg_y(0,0)\right)^2 - 4j_0L}\right),$$

where $L = L_{S_0}(0)$.

(i) According to Theorem 3.4, if a trajectory hits the line $f = 0$ sufficiently close to the zero equilibrium, then the trajectory converges to this equilibrium. In particular, if $f_x(0,0) + L_{S_0}(x_0)g_y(0,0) > -\sqrt{j_0 L_{S_0}(x_0)}$ for a small x_0 and $S_0 \in \Sigma_\nu$, then, due to condition (3.3), the zero equilibrium of system (4.8) is either a focus or a center, hence a trajectory $(x(t), y(t))$ starting sufficiently close to zero must hit the line $f = 0$. In the complementary case $f_x(0,0) + L_{S_0}(x_0)g_y(0,0) \leqslant -\sqrt{j_0 L_{S_0}(x_0)}$, the zero equilibrium of system (4.8) is exponentially stable, hence the trajectory either hits the line $f = 0$ or converges to zero without hitting the line $f = 0$.

(ii) Fix an $\widetilde{L}$ satisfying (3.4). The definition of $L_{\max}, L^\nu_{\min}$ implies that for any sufficiently small $\tilde{x}$ there is a staircase state $\widetilde{S}_0 \in \Sigma_\nu$ with the end at the point $(\tilde{x}, \tilde{x})$ such that $L_{\widetilde{S}_0}(\tilde{x}) = \widetilde{L}$. To be definite, assume that the initial segment of all such states is horizontal and that the domain $f > 0$ is situated below the line $f = 0$ on the (x, y) phase plane. Consider a point $(\tilde{x}, \tilde{y})$ on the line $f(x, y) = 0$, $g(x, y) > 0$ with an arbitrarily small $\tilde{x} \neq 0$.[5] If a point (x_0, y_0) lies below the line $f = 0$ sufficiently close to the point $(\tilde{x}, \tilde{y})$ and $S_0 \in \Sigma_\nu$ is sufficiently close to $\widetilde{S}_0$, then the trajectory of system (4.8) starting from the point (x_0, y_0) goes almost vertically up and hits the line $f = 0$. This trajectory is also a trajectory of system (1.7) for small x_0, as the second segment of the state S_0 has the length $l > \nu$. Hence, all such trajectories of system (1.7) hit the line $f = 0$ and according to Theorem 3.4 converge to the zero equilibrium. This proves condition (a) of the definition of the partial stability. To prove condition (b), consider that if $S_0 \in \Sigma_\nu$ is close to $\widetilde{S}$, then the zero equilibrium is an unstable node with the Lyapunov exponents $\lambda_1 > \lambda_2 > 0$ for system (4.8) due to assumption (3.4). It is straightforward to check that the eigenvector e_1 corresponding to the eigenvalue λ_1 is transversal to the line $f = 0$. Hence a trajectory of system (4.8) with $S_0 = \widetilde{S}$ starting at a point $(\tilde{x}, \tilde{y}) = re_1$ with an arbitrarily small $r \neq 0$ from the domain $f > 0$ leaves some fixed neighbourhood U of zero without hitting the line $f = 0$. The same is true for every trajectory of system (4.8) with $S_0 \in \Sigma_\nu$ sufficiently close to $\widetilde{S}$, which starts from a point (x_0, y_0) sufficiently close to $(\tilde{x}, \tilde{y})$. As these trajectories do not intersect the line $f = 0$ in U, they are also trajectories of system (1.7) with the admissible initial Preisach state. This proves condition (b).

[5] In the case when the domain $f > 0$ is situated above the line $f = 0$, we would consider a point $(\tilde{x}, \tilde{y})$ on the line $f = 0$, $g < 0$ instead. If the initial segment of the state S_0 is vertical, then the domain $f > 0$ should be replaced with the domain $f < 0$ in the above argument.

(iii) This case is similar to (ii). Here condition (3.5) ensures that there is an admissible state $\widetilde{S}_0 \in \Sigma_\nu$ such that the zero equilibrium of system (4.8) with any $S_0 \in \Sigma_\nu$ sufficiently close to $\widetilde{S}_0$ is a stable node with eigenvalues $\lambda_2 < \lambda_1 < 0$ and eigenvectors e_1, e_2. Hence, trajectories of (4.8) which start sufficiently close to the straight line going through the origin in the direction of the eigenvector e_1 converge to zero without crossing the line $f = 0$. The same is therefore true for trajectories of system (1.7) if an admissible initial Preisach state is chosen as in the case (ii). At the same time, there is a set of trajectories of system (1.7) starting sufficiently close to the line $f = 0$ that hit this line. According to Theorem 3.2 they escape some fixed vicinity of zero.

(iv) This case is a counterpart of (i). If a trajectory $(x(t), y(t))$ hits the line $f = 0$, then it escapes some neighbourhood U of the zero equilibrium due to Theorem 3.2. In particular, if $f_x(0,0) + L_{S_0}(x_0)g_y(0,0) < \sqrt{j_0 L_{S_0}(x_0)}$, then, due to condition (3.6), the zero equilibrium of system (4.8) is either a focus or a center, hence the trajectory $(x(t), y(t))$ must hit the line $f = 0$. If $f_x(0,0) + L_{S_0}(x_0)f_y(0,0) \geqslant \sqrt{j_0 L_{S_0}(x_0)}$, then the zero equilibrium of system (4.8) is an unstable node, hence the trajectory either hits the line $f = 0$ or escapes U without hitting the line $f = 0$.

(v) If a trajectory does not hit the line $f = 0$, then, due to the condition $j_0 < 0$, it is a trajectory of the ordinary differential system (4.8) with a saddle equilibrium point at the origin. Hence, the trajectory escapes some neighbourhood U of the origin (except if the initial point (x_0, y_0) belongs to the stable manifold of the equilibrium). If a trajectory hits the line $f = 0$, then it escapes U due to Theorems 3.2, 3.3. $\square$

References

[1] *B. Appelbe, D. Rachinskii, A. Zhezherun*: Hopf bifurcation in a van der Pol type oscillator with magnetic hysteresis. Physica B *403* (2008), 301–304.

[2] *B. Appelbe, D. Flynn, H. McNamara, J. P. O'Kane, A. Pimenov, A. Pokrovskii, D. Rachinskii, A. Zhezherun*: Rate-independent hysteresis in terrestrial hydrology. IEEE Control Syst. Mag. *29* (2009), 44–69.

[3] *Z. Balanov, W. Krawcewicz, D. Rachinskii, A. Zhezherun*: Hopf bifurcation in symmetric networks of coupled oscillators with hysteresis. J. Dyn. Differ. Equations *24* (2012), 713–759.

[4] *A.-L. Bessoud, U. Stefanelli*: Magnetic shape memory alloys: three-dimensional modeling and analysis. Math. Models Methods Appl. Sci. *21* (2011), 1043–1069.

[5] *M. Brokate, J. Sprekels*: Hysteresis and Phase Transitions. Applied Mathematical Sciences 121, Springer, New York, 1996.

[6] *M. Brokate, A. V. Pokrovskii, D. Rachinskii, O. Rasskazov*: Differential equations with hysteresis via a canonical example. The Science of Hysteresis. Vol. I (G. Bertotti et al., eds.). Mathematical modeling and applications, Elsevier, Academic Press, Amsterdam, 2006, pp. 125–291.

[7] *M. Brokate, A. Pokrovskii, D. Rachinskii*: Asymptotic stability of continuum sets of periodic solutions to systems with hysteresis. J. Math. Anal. Appl. *319* (2006), 94–109.

[8] *M. Brokate, S. MacCarthy, A. Pimenov, A. Pokrovskii, D. Rachinskii*: Modelling energy dissipation due to soil-moisture hysteresis. Environ Model Assess *16* (2011), 313–333.
[9] *J. Cagnol, B. Miara, A. Mielke, G. Stavroulakis*: State of the Art, Trends, and Directions in Smart Systems. www.wias-berlin.de/people/mielke/papers/stateoftheart.pdf.
[10] *D. Cellai, A. Lawlor, K. A. Dawson, J. P. Gleeson*: Tricritical point in heterogeneous k-core percolation. Phys. Rev. Lett. *107* (2011), no. 175703, 5 pages.
[11] *R. Cross, H. McNamara, A. Pokrovskii, D. Rachinskii*: A new paradigm for modelling hysteresis in macroeconomic flows. Physica B *403* (2008), 231–236.
[12] *R. Cross, H. McNamara, A. Pokrovskii*: Modelling macroeconomic flows related to large ensembles of elementary exchange operations. Physica B *403* (2008), 451–455.
[13] *R. Cross, H. McNamara, A. Pokrovskii*: Memory of recessions. Strathclyde discussion papers in economics (2010), no. 10–09, 26 pages.
[14] *R. Cross, H. McNamara, L. Kalachev, A. Pokrovskii*: Hysteresis in the fundamentals of macroeconomics. Strathclyde discussion papers in economics (2010), no. 10–08, 35 pages.
[15] *R. Cross*: On the foundations of hysteresis in economic systems. Economics and Philosophy *9* (1993), 53–74.
[16] *R. Cross, M. Grinfeld, H. Lamba*: Hysteresis and economics. IEEE Control Syst. Mag. *29* (2009), 30–43.
[17] *R. Cross, H. McNamara, L. Kalachev, A. Pokrovskii*: Hysteresis and post Walrasian economics. Discrete Contin. Dyn. Syst., Ser. B *18* (2013), 377–401.
[18] *K. Dahmen, Y. Ben-Zion*: Jerky motion in slowly driven magnetic and earthquake fault systems, physics of. Encyclopedia of Complexity and Systems Science (C. Marchetti, R. A. Meyers, eds.). Springer, 2009, pp. 5021–5037.
[19] *D. Davino, A. Giustiniani, C. Visone*: Compensation and control of two-inputs systems with hysteresis. J. Phys.: Conf. Ser. *268* (2011), no. 12005, 16 pages.
[20] *P. Diamond, D. Rachinskii, M. Yumagulov*: Stability of large cycles in a nonsmooth problem with Hopf bifurcation at infinity. Nonlinear Anal., Theory Methods Appl. *42* (2000), 1017–1031.
[21] *P. Diamond, N. Kuznetsov, D. Rachinskii*: On the Hopf bifurcation in control systems with a bounded nonlinearity asymptotically homogeneous at infinity. J. Differ. Equations *175* (2001), 1–26.
[22] *D. Ekanayake, R. V. Iyer*: Asymptotic behavior of a low dimensional model for magnetostriction for periodic inputs. Physica B: Physics of Condensed Matter *403* (2008), 257–260.
[23] *M. Eleuteri, L. Lussardi, U. Stefanelli*: A rate-independent model for permanent inelastic effects in shape memory materials. Netw. Heterog. Media (electronic only) *6* (2011), 145–165.
[24] *M. Eleuteri, J. Kopfová, P. Krejčí*: Magnetohydrodynamic flow with hysteresis. SIAM J. Math. Anal. *41* (2009), 435–464.
[25] *D. Flynn, H. McNamara, J. P. O'Kane, A. Pokrovskii*: Application of the Preisach model to soil-moisture hysteresis. The Science of Hysteresis Vol. III (G. Bertottiand, I. D. Mayergoyz, eds.). Hysteresis in materials, Elsevier, Academic Press, Amsterdam, 2006, pp. 689–744.
[26] *D. Flynn, A. Zhezherun, A. Pokrovskii, J. P. O'Kane*: Modeling discontinuous flow through porous media using ODEs with Preisach operator. Physica B *403* (2008), 440–442.
[27] *J. P. Gleeson*: High-accuracy approximation of binary-state dynamics on networks. Phys. Rev. Lett. *107* (2011), no. 068701, 9 pages.
[28] *M. Göcke*: Various concepts of hysteresis applied in economics. Journal of Economic Surveys *16* (2002), 167–188.

[29] *D. Goulding, S. P. Hegarty, O. Rasskazov, S. Melnik, M. Hartnett, G. Greene, J. G. McInerney, D. Rachinskii, G. Huyet*: Excitability in a quantum dot semiconductor laser with optical injection. Phys. Rev. Lett. *98* (2007), no. 153903, 4 pages.
[30] *A. Ivanyi* (ed.): Preisach Memorial Book. Akademiai Kiado, Budapest, 2005.
[31] *R. V. Iyer, X. Tan, P. S. Krishnaprasad*: Approximate inversion of the Preisach hysteresis operator with application to control of smart actuators. IEEE Trans. Automat. Control *50* (2005), 798–810.
[32] *B. Jayawardhana, H. Logemann, E. P. Ryan*: Infinite-dimensional feedback systems: the circle criterion and input-to-state stability. Commun. Inf. Syst. *8* (2008), 413–444.
[33] *A. M. Krasnosel'skii, D. Rachinskii*: On a bifurcation governed by hysteresis nonlinearity. NoDEA, Nonlinear Differ. Equ. Appl. *9* (2002), 93–115.
[34] *M. Krasnosel'skii, A. Pokrovskii*: Systems with Hysteresis. Translated from the Russian by Marek Niezgódka, Springer, Berlin, 1989.
[35] *B. Krauskopf, K. R. Schneider, J. Sieber, S. M. Wieczorek, M. Wolfrum*: Excitability and self-pulsations near homoclinic bifurcations in semiconductor laser systems. Optics Communications *215* (2003), 367–379.
[36] *P. Krejčí*: On Maxwell equations with the Preisach hysteresis operator: The one-dimensional time-periodic case. Apl. Mat. *34* (1989), 364–374.
[37] *P. Krejčí, J. P. O'Kane, A. Pokrovskii, D. Rachinskii*: Mathematical models of hydrological systems with Preisach hysteresis. Physica D *241* (2012), 2010–2028.
[38] *P. Krejčí, J. P. O'Kane, A. Pokrovskii, D. Rachinskii*: Stability results for a soil model with singular hysteretic hydrology. J. Phys.: Conf. Ser. *268* (2011), no. 012016, 19 pages.
[39] *P. Krejčí*: Resonance in Preisach systems. Appl. Math., Praha *45* (2000), 439–468.
[40] *K. Kuhnen, P. Krejčí*: Compensation of complex hysteresis and creep effects in piezoelectrical actuated systems—a new Preisach modeling approach. IEEE Trans. Automat. Control *54* (2009), 537–550.
[41] *H. Lamba, M. Grinfeld, S. McKee, R. Simpson*: Subharmonic ferroresonance in an LCR circuit with hysteresis. IEEE Transactions on Magnetics *33* (1997), 2495–2500.
[42] *H. Lamba, S. McKee, R. Simpson*: The effect of circuit parameters on ferroresonant solutions in an LCR circuit. J. Phys. A, Math. Gen. *31* (1998), 7065–7076.
[43] *I. D. Mayergoyz*: Mathematical Models of Hysteresis. Springer, New York, 1991.
[44] *I. D. Mayergoyz, G. Bertotti* (eds.): The Science of Hysteresis. Vol. III. Hysteresis in materials, Elsevier, Academic Press, Amsterdam, 2006.
[45] *S. McCarthy, D. Rachinskii*: Attempts at a numerical realisation of stochastic differential equations containing Preisach operator. J. Phys.: Conf. Ser. *268* (2011), no. 012019, 15 pages.
[46] *J. P. O'Kane*: The hysteretic linear reservoir—a new Preisach model. Physica B: Condensed Matter *372* (2006), 388–392.
[47] *J. P. O'Kane*: Hysteresis in hydrology. Acta Geophys. Pol. *53* (2005), 373–383.
[48] *J. P. O'Kane*: The FEST model-a test bed for hysteresis in hydrology and soil physics. J. Phys.: Conf. Ser. *22* (2005), 148–163.
[49] *J. P. O'Kane, A. Pokrovskii, P. Krejčí, R. Haverkamp*: Hysteresis and terrestrial hydrology. EGS-AGU-EUG Joint Assembly *1* (2003), 6154.
[50] *A. Pimenov, D. Rachinskii*: Linear stability analysis of systems with Preisach memory. Discrete Contin. Dyn. Syst., Ser. B *11* (2009), 997–1018.
[51] *A. Pimenov, T. C. Kelly, A. Korobeinikov, M. J. A. O'Callaghan, A. Pokrovskii, D. Rachinskii*: Memory effects in population dynamics: spread of infectious disease as a case study. Math. Model. Nat. Phenom. *7* (2012), 1–30.
[52] *A. Pimenov, T. C. Kelly, A. Korobeinikov, M. J. O'Callaghan, A. Pokrovskii*: Systems with hysteresis in mathematical biology via a canonical example. Mathematical Model-

ing, Clustering Algorithms and Applications (C. L. Wilson, ed.). Nova Science Publishers, 2010.
[53] *G. S. Sander, O. J. Glidewell, J. Norbury*: Dynamic capillary pressure, hysteresis and gravity-driven fingering in porous media. J. Phys.: Conf. Ser. *138* (2008), no. 012023, 14 pages.
[54] *J. P. Sethna, K. A. Dahmen, O. Perković*: Random-field Ising models of hysteresis. The science of Hysteresis Vol. II (G. Bertotti, I. Mayergoyz, eds.). Physical modeling, micromagnetics, and magnetization dynamics, Elsevier, Academic Press, Amsterdam, 2006, pp. 107–179.
[55] *P.D. Spanos, P. Cacciola, G. Muscolino*: Stochastic averaging of Preisach hysteretic systems. J. Eng. Mech. *130* (2004), 1257–1267.
[56] *D. Rachinskii*: Asymptotic stability of large-amplitude oscillations in systems with hysteresis. NoDEA, Nonlinear Differ. Equ. Appl. *6* (1999), 267–288.
[57] *A. Rezaei-Zare, M. Sanaye-Pasand, H. Mohseni, S. Farhangi, R. Iravani*: Analysis of ferroresonance modes in power transformers using Preisach-type hysteretic magnetizing inductance. IEEE Trans. Power Deliv. *22* (2007), 919–929.
[58] *A. Visintin*: Differential Models of Hysteresis. Applied Mathematical Sciences 111, Springer, Berlin, 1994.
[59] *C. Visone*: Hysteresis modelling and compensation for smart sensors and actuators. J. Phys.: Conf. Ser. *138* (2008), no. 012028, 24 pages.
[60] *Y. Wang, Z. G. Ying, W. Q. Zhu*: Nonlinear stochastic optimal control of Preisach hysteretic systems. Probabilistic Engineering Mechanics *24* (2009), 255–264.

Authors' addresses: *Stephen McCarthy*, Department of Applied Mathematics, University College Cork, Cork, Ireland, *Dmitrii Rachinskii*, Department of Applied Mathematics, University College Cork, Cork, Ireland & Department of Mathematical Sciences, University of Texas at Dallas, USA, e-mail: `d.rachinskii@ucc.ie`, `dmitry.rachinskiy@utdallas.edu`.